Josef Stefan Institute Seminar

The Belle II Pixel Detector, search for the rare charm decays $D^0 \to \pi^0 l^+ l^-$ in Belle and studies with displaced vertices in early Belle II data

March 22, 2021

Varghese Babu
DESY, Hamburg

Outline

- The Belle II Pixel detector
- Search for the rare charm decays $D^0 \to \pi^0 l^+ l^-$ in Belle
- Studies with displaced vertices in early Belle II data.

The Belle II Pixel detector

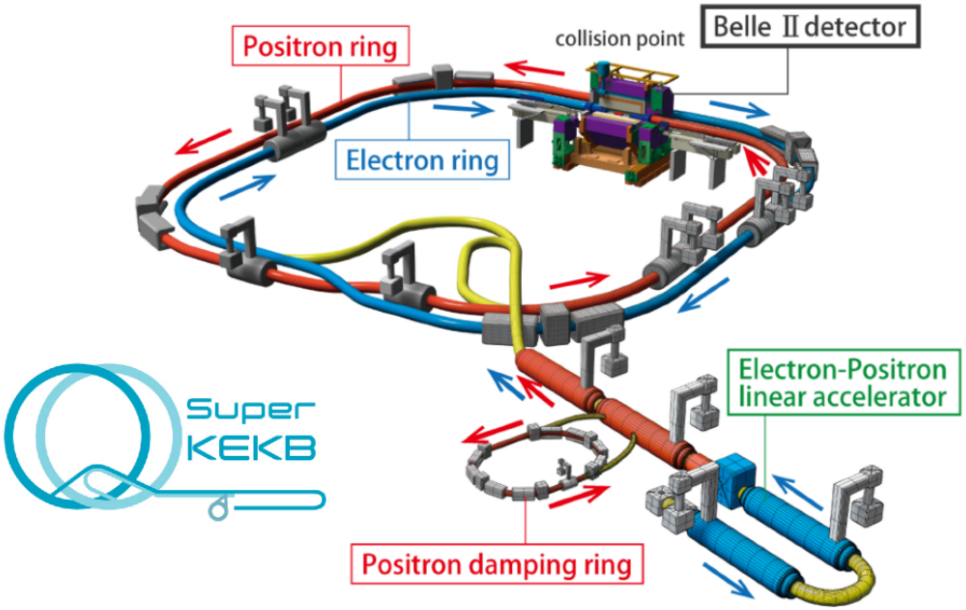

Belle II Detector

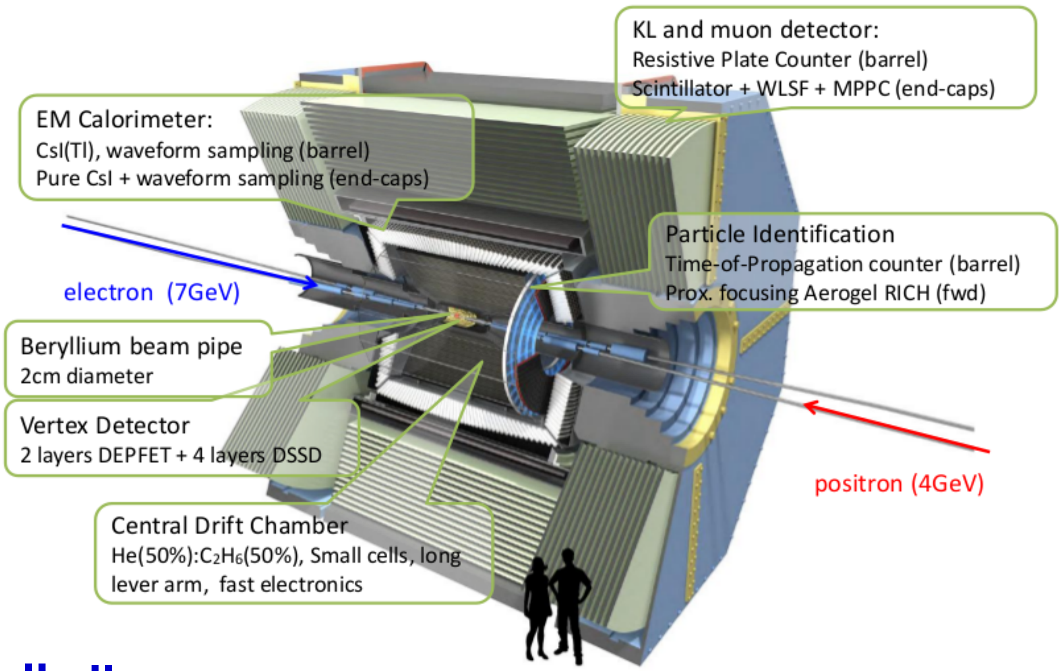

Super KEKB

- asymmetric $e^+ e^-$ collider
- $E_{cm} = M_{Y(4S)} \approx 10.58$ GeV ⇒ “B factory”
- goal: L peak = 6×10^{35} cm^{-2} s^{-1}
  - ➔ “nano-beam” scheme and increased currents
  - ➔ 2.4×10^{34} cm^{-2} s^{-1} achieved on June 21, 2020

Belle II

- target L_{int} : 50 ab^{-1} by ~2030/2031
  - ➔ physics data-taking with full setup since March 2019
  - ➔ 90 fb^{-1} recorded by end of 2020
- upgraded trigger rate: 30 kHz
- upgraded detectors

Belle II Vertex Detector (VXD)

● **acceptance**

17° < Θ < 150°, $p_T \gtrsim$ 40 MeV

● **Silicon Vertex Detector (SVD)**

4 layers of 2-sided silicon strips, r ≤ 140 mm

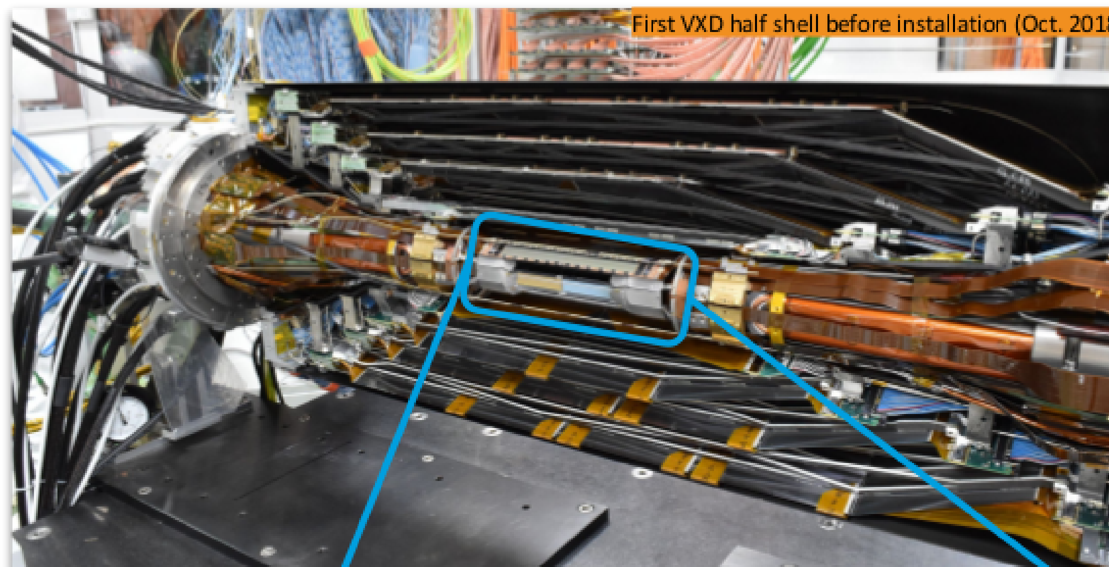

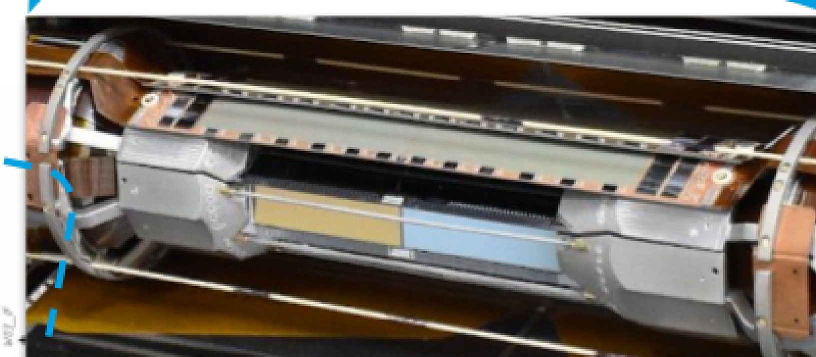

● **Pixel Vertex Detector (PXD)**

2 layers at radii 14 mm and 22 mm

8 inner + 12 outer module-pairs (“ladders”)

⇒ only 8 (inner) + 2 (outer) ladders installed

~7.7 x 10^6 pixels

50 µm x 55-85 µm pitch (varies in layers along z)

~0.21 % X_0 / layer material budget

20 µs integration time

< 3 % occupancy (< 0.5 hits/µm^2 /s)

to withstand 20 Mrad over 10 years

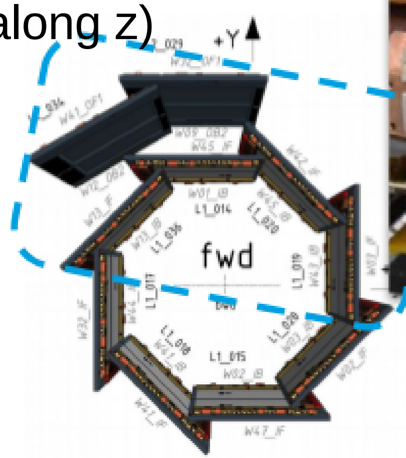

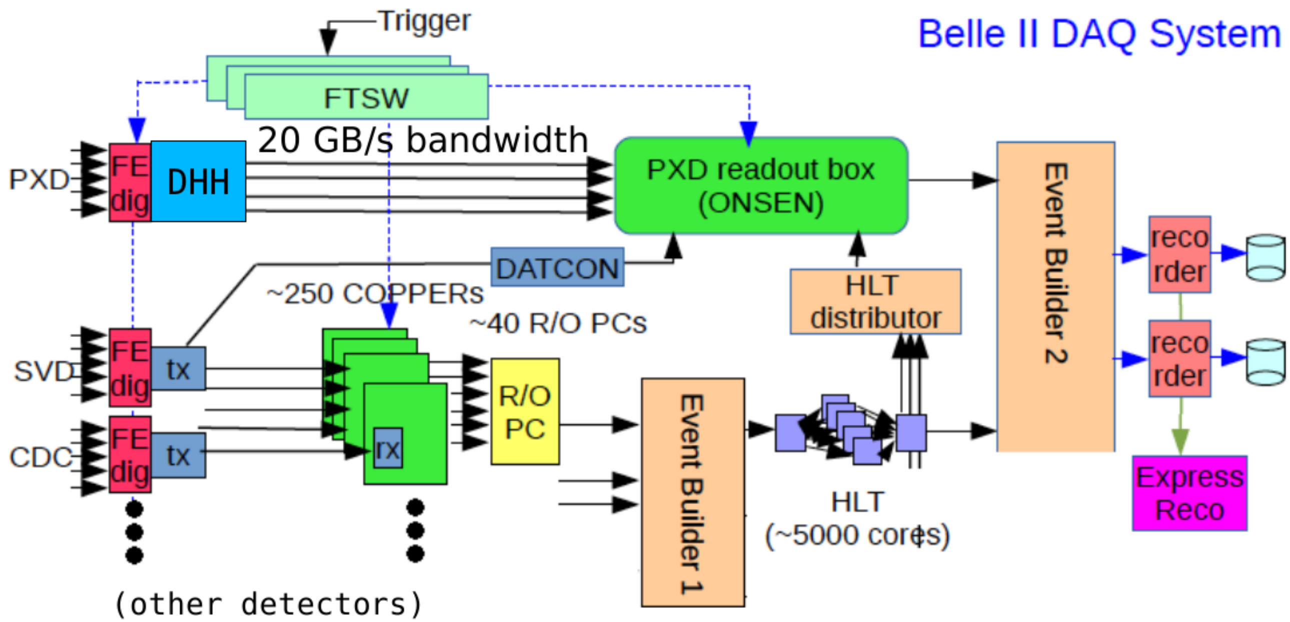

Track reconstruction and PXD role

- PXD DAQ separated from rest of Belle II
  - ➔ produces 10x data of rest of Belle II
  - ➔ track finding seeded in CDC (pT > 100 MeV) or else SVD
  - ➔ HLT: extrapolates tracks to “regions of interest” on PXD
  - ➔ only those PXD hits are stored and used in track fit

- PXD layer one crucial for impact parameter resolution

- PXD layer two (will be) crucial for handling background

Working principle:

● Field Effect Transistor (FET) on top of fully depleted silicon bulk

➔ gate voltage regulates source→drain current

● internal gate: n-implant below FET gate

➔ collects free charge carriers to modulate drain current

● periodic active clearing of internal gate achieved via clear implant (n+) and “punch through” mechanism

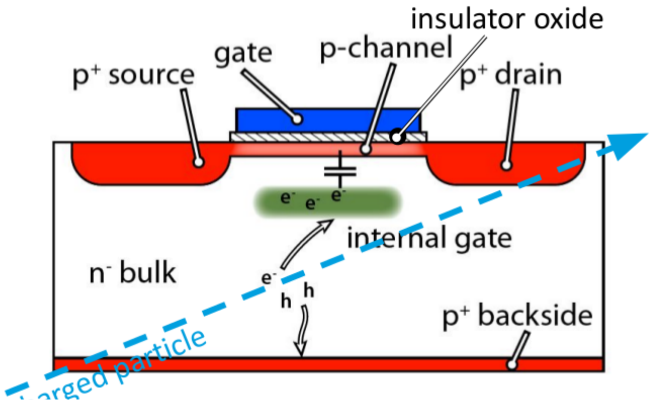

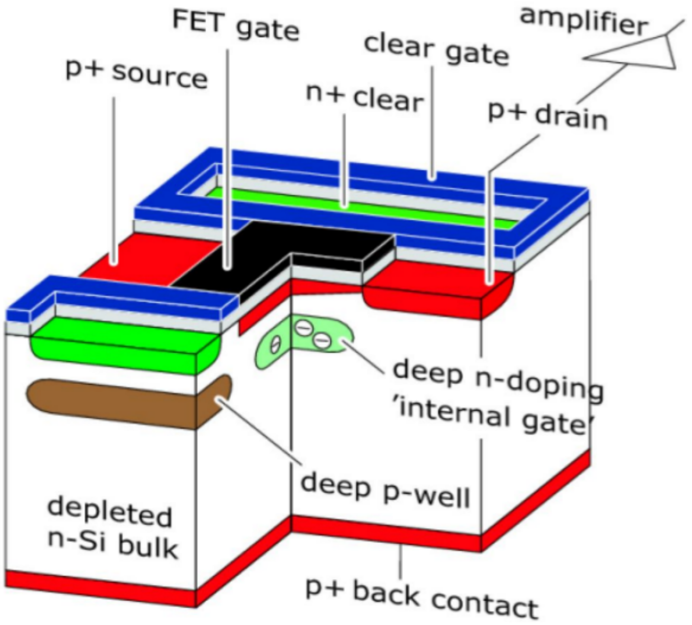

Characteristics:

● fast charge collection (O(ns))

● non-destructive signal readout

● internal amplification $g_q \approx 500$ pA/e⁻

● high signal-to-noise ratio

● low power consumption

● thin sensors (75 μm in active region: DEPFET matrix)

PXD modules

- 75µm thin sensors
- Rolling shutter read-out → low power

- 50kHz → 20 µs integration time
- Design: 1% occupancy in layer 1
- ➔ 3% occupancy limit (DHP, DAQ, Tracking)

- Rad. hard sensor and ASICSs
- 40 sensors, 250x768 pixels each

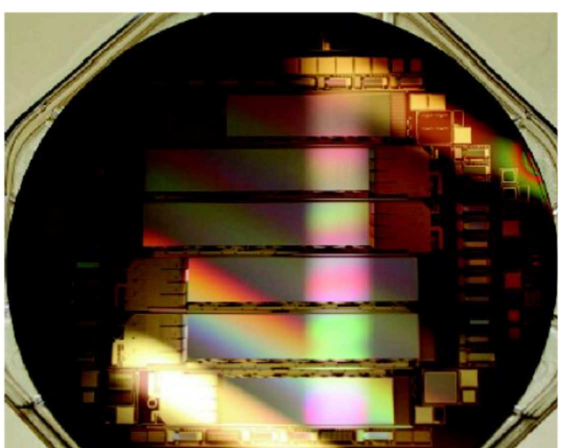

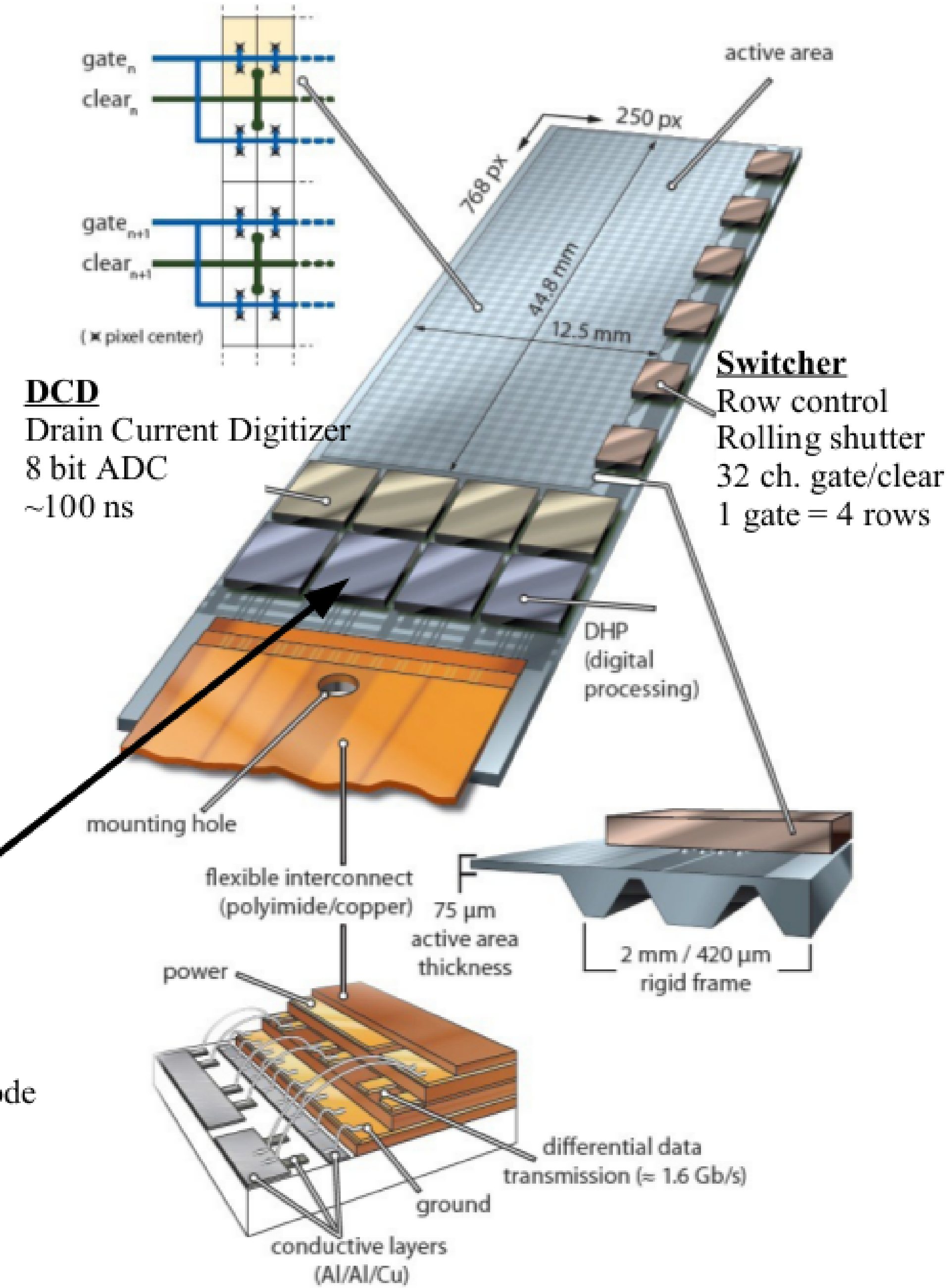

DHP
Digital processing
Zero suppression
Pedestal and common mode correction
Trigger and timing

Readout and Calibration

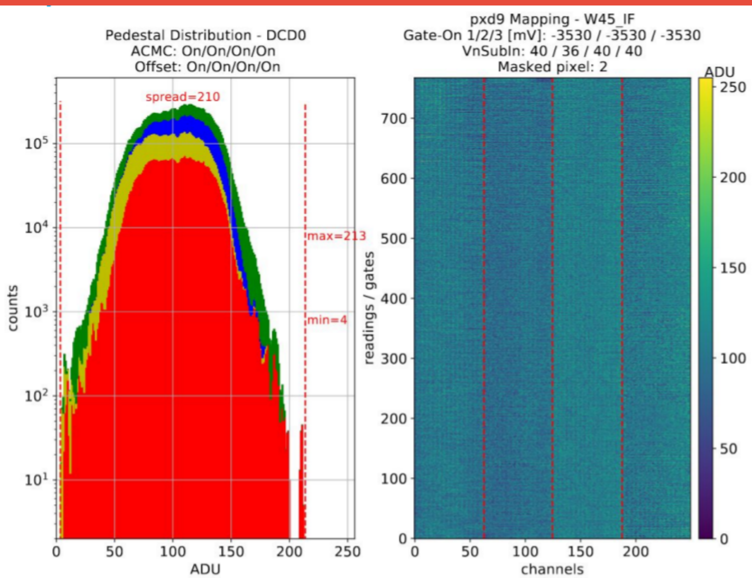

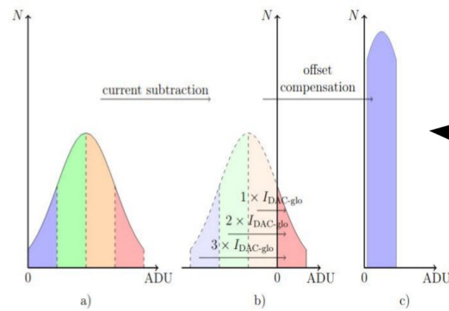

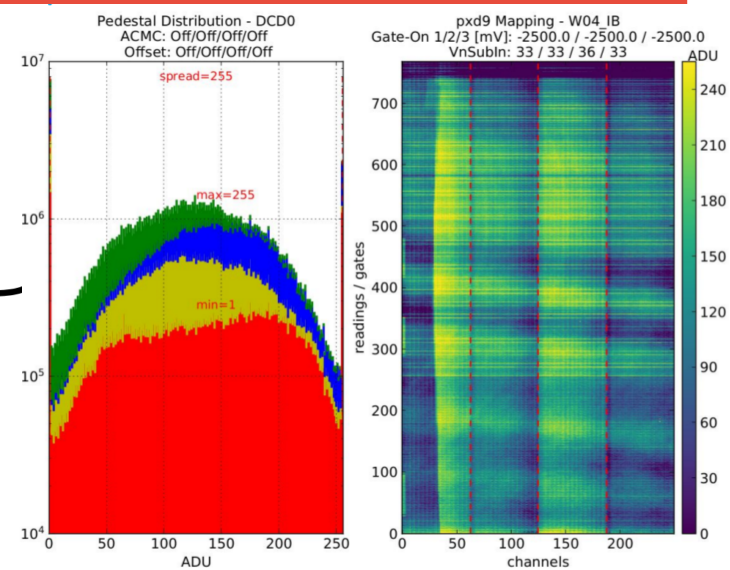

rolling shutter mode

- signals read gate by gate
- read-clear cycle in ~100 ns

➔ full integration time 20 µs (1 “frame”)

➔twice SuperKEKB revolution time

sampling:

- drain currents measured once
- pedestal correction on DHP
- zero suppression:
  - ➔ only signals above threshold send out

Calibration

- median current for every pixel and store on DHP
  - ➔ values subtracted from every subsequent measurement on DHP
  - ➔ values updated regularly during operation
- various current offsets in DCDs allow pixel-wise pedestal compression
  - ➔ sensor homogenization

Support and Cooling Block (SCB)

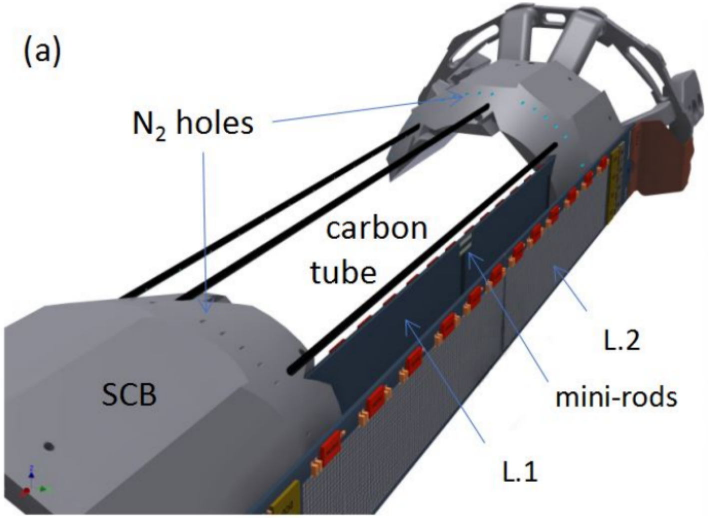

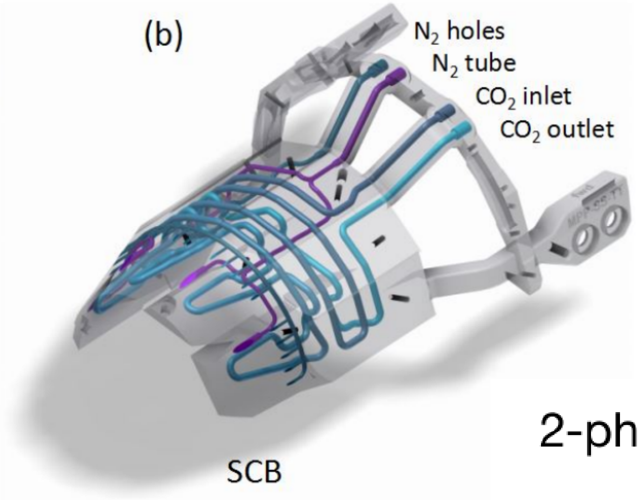

2-phase CO_2 cooling

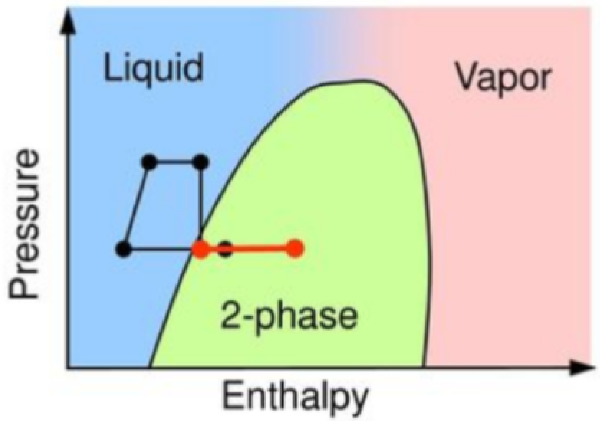

2PACL: 2-Phase Accumulator Controlled Loop

- **The power consumption of full PXD is 420W**
  - 360W are contributed from DCD/DHP, which are located in the end of stave.
  - Active 2 phase CO2 cooling is required there.

- **Little power from matrix (0.5W per module) and Switchers (1W per module)**
  - Air cooling is sufficient in the sensitive area.

VXD Installation 2018

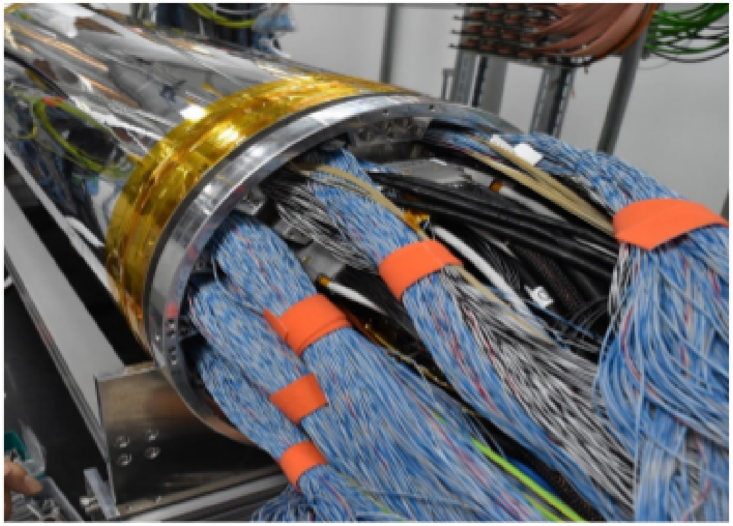

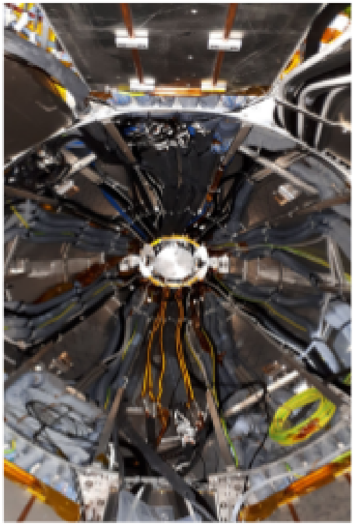

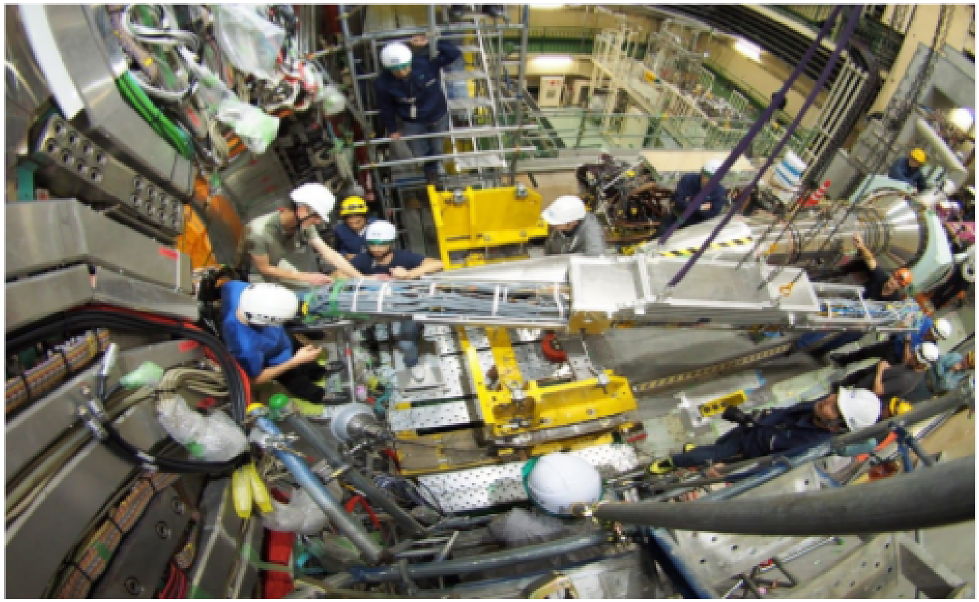

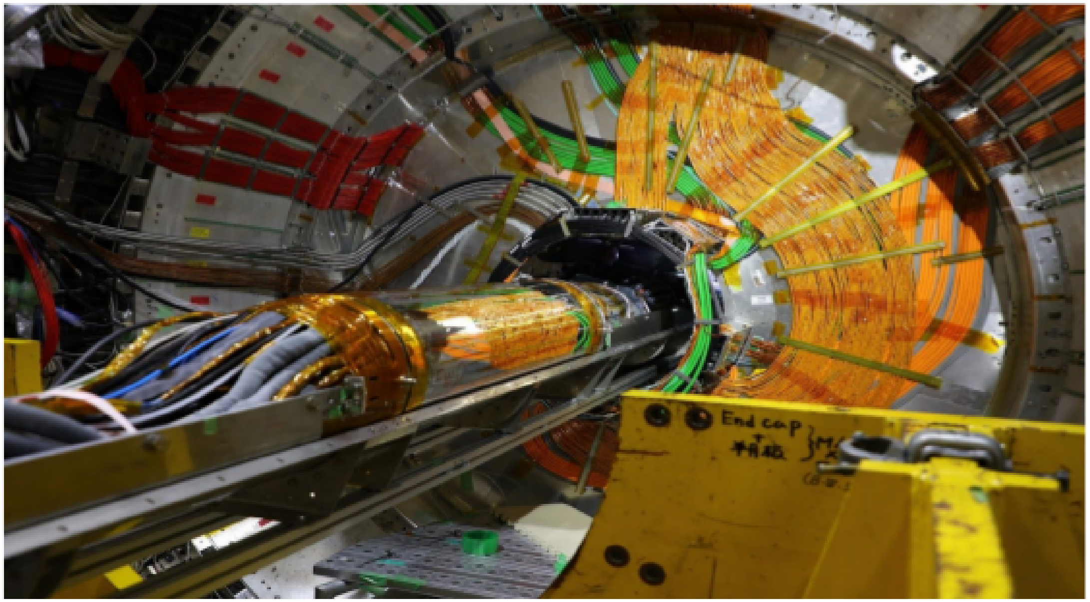

PXD Performance in Belle II

cluster charge distribution

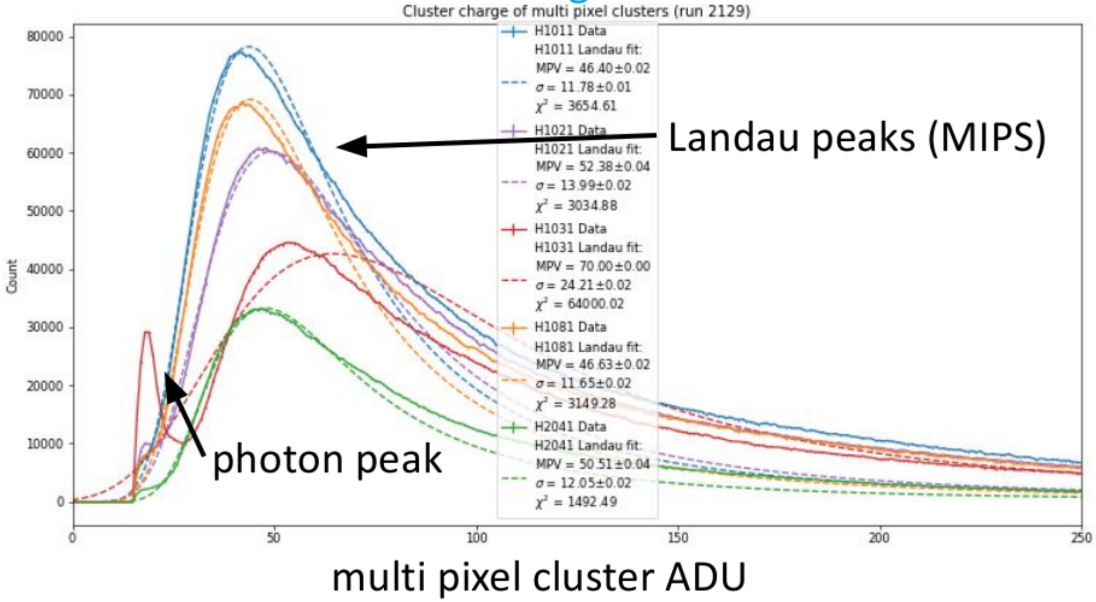

noise distribution

(pedestal fluctuations)

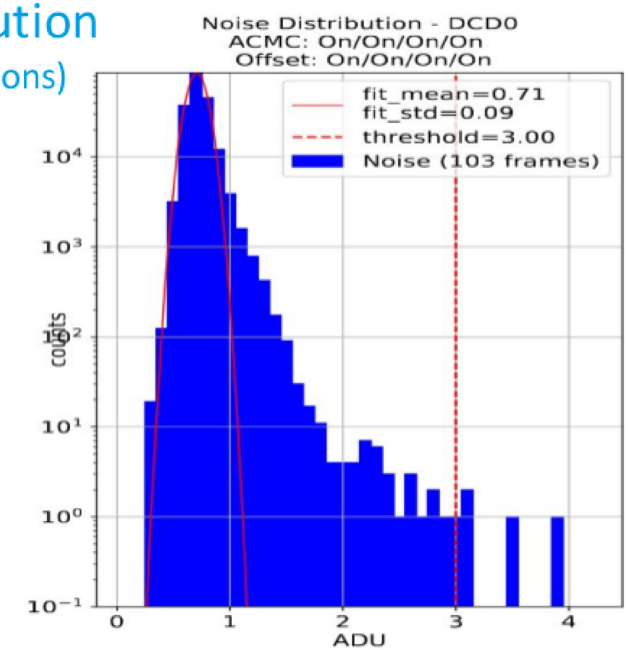

- noise performance < 1 ADU (∼200 e⁻)
- at a SNR of ∼30 - 50
- homogeneous noise and signal response across module matrix

cluster charge MPV

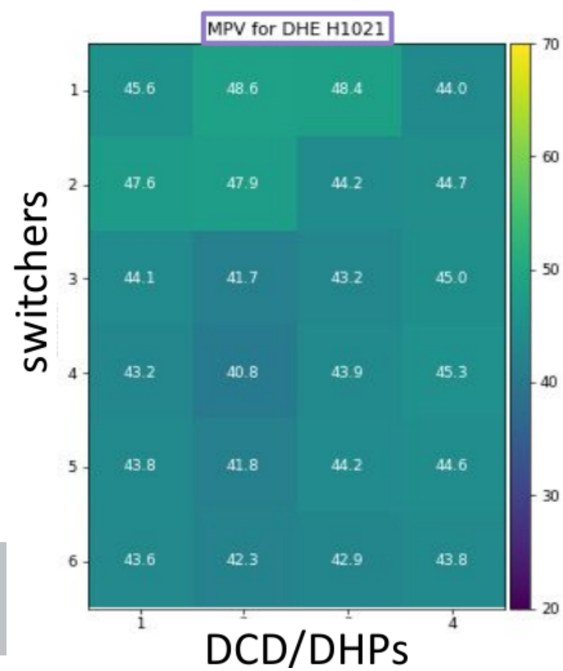

SNR MPV

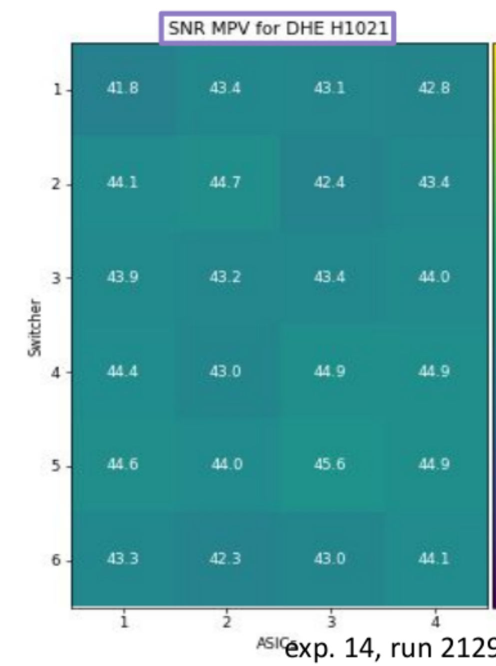

PXD Performance in Belle II
~98% hit-efficiency

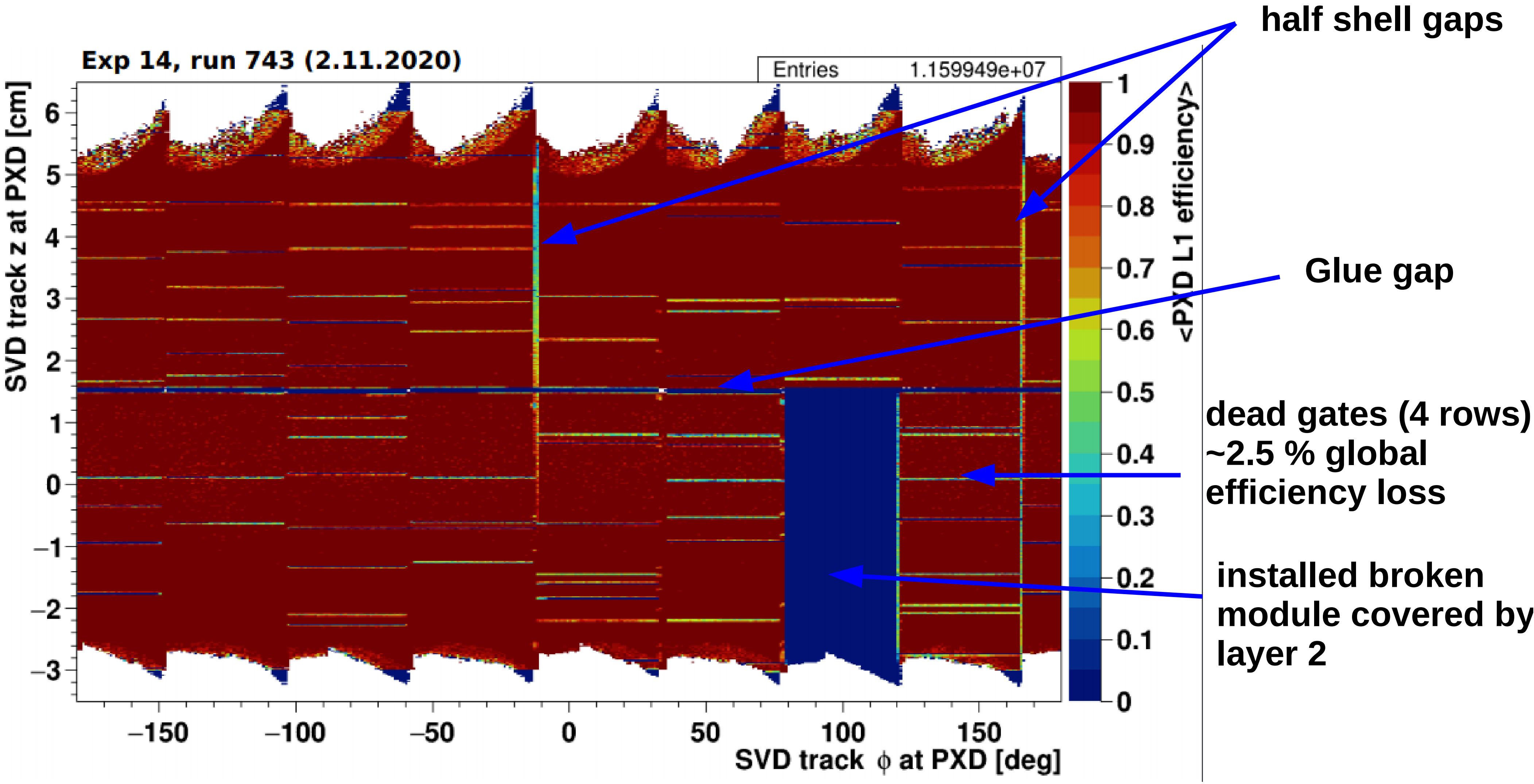

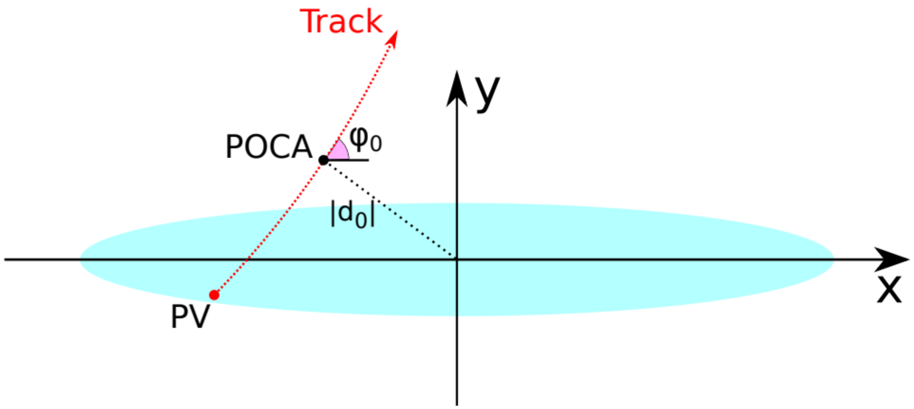

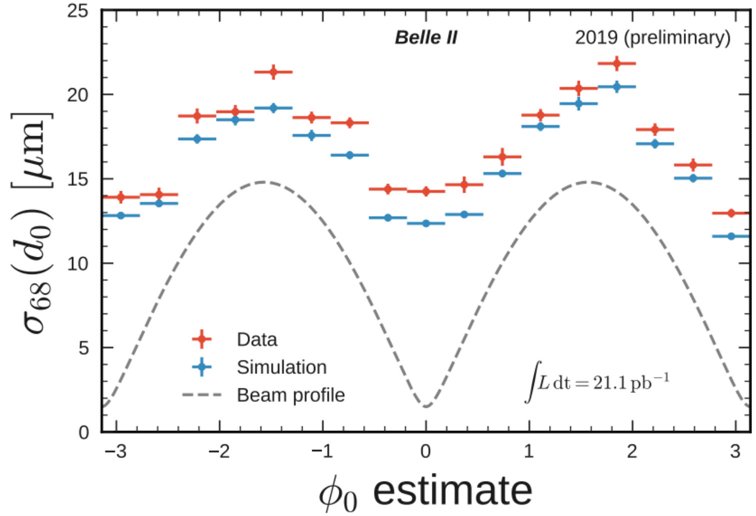

- resolution improvement visible at $t < 0$:

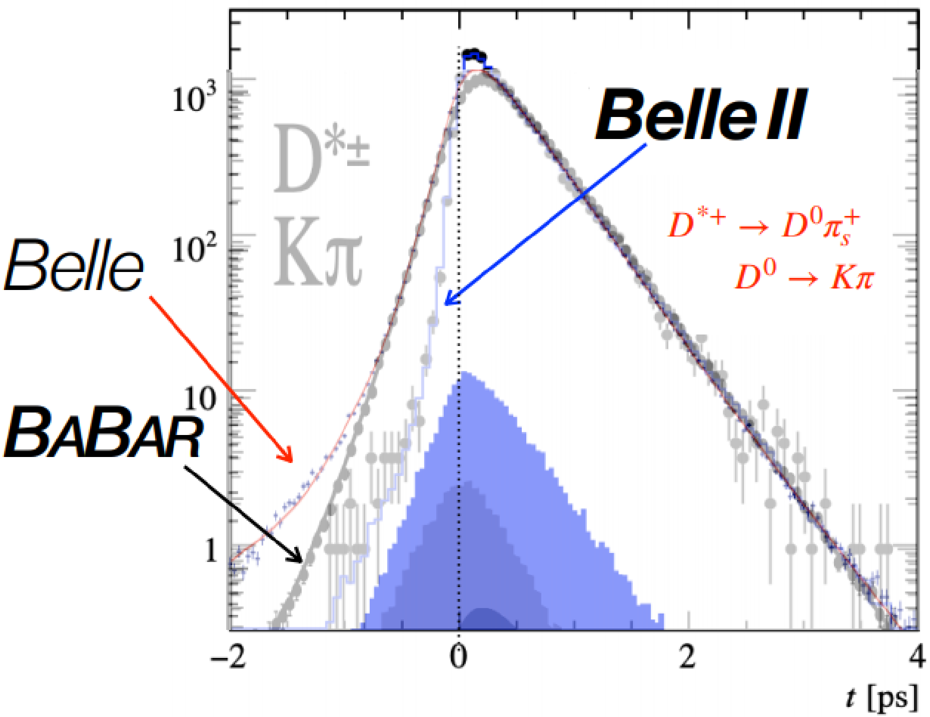

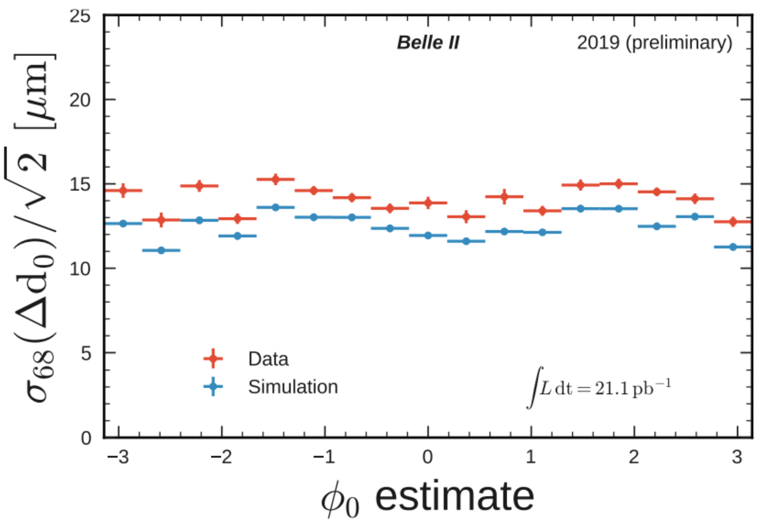

- resolution: 1.5 - 2 x better than Belle

	Data	Simulation
$\hat{\sigma}(d_0)$ [μm]	$14.2 \pm 0.1\,(\mathrm{stat}) \pm 0.1\,(\mathrm{syst})$	$12.5 \pm 0.1\,(\mathrm{stat})$
$\hat{\sigma}(z_0)$ [μm]	$16.1 \pm 0.1\,(\mathrm{stat}) \pm 0.1\,(\mathrm{syst})$	$13.9 \pm 0.1\,(\mathrm{stat})$

- Proper time resolution at BelleII is a factor 2 better than Belle & BABAR thanks to a betterperforming vertex detector

Search for the rare decays $D^0 \to \pi^0 l^+l^-$ in Belle

Search for the rare decays $D^0 \rightarrow \pi^0 l^+ l^-$ in Belle (Presentation)

- Decays driven by flavor changing neutral currents (FCNC) are highly suppressed in the standard model and occur only at one-loop level.

- Since the loop may be mediated by virtual particles and forces beyond the standard model, this makes is a great testing ground for new physics.

- The FCNC transition b → sll has garnered significant interest of recent with LHCb reporting several anomalies. An example is the well known observation

$$R_K = 0.846 +0.060+0.016-0.054-0.014$$

R. Aaij et al. (LHCb Collaboration) Phys. Rev. Lett. 122, 191801 – Published 13 May 2019

Search for the rare decays $D^0 \rightarrow \pi^0 l^+ l^-$ in Belle

- The charm quark is the only charge 2/3 quark which allows investigations of unusual couplings.

- For the FCNC transition $c \rightarrow ull$, the long distance contribution is expected to dominate over the short distance contributions.

- The SM branching fraction for the $D^0 \rightarrow \pi^0 ll$ modes are calculated to be 2.1×10^{-7} S. Fajfer, S. Prelovsek, and P. Singer, Phys. Rev. D 64, 114009 - Published 7 November 2001

Previous measurements

$$B(D^0 \rightarrow \pi^0 e^+ e^-) < 4 \times 10^{-6} \text{ (90\% C.L.)}$$

M. Ablikim et. al., Phys.Rev.D 97 (2018) 7, 072015, arXiv:1802.09752 (BES3 Collaboration)

$$B(D^0 \rightarrow \pi^0 \mu^+ \mu^-) < 1.8 \times 10^{-4} \text{ (90\% C.L.)}$$

K. Kodama et. al., Phys.Lett.B 345 (1995) 85-92 (E653 Collaboration)

Search for the rare decays $D^0 \to \pi^0 l^+ l^-$ in Belle

Table: Preselection cuts.

Variable	Cut
E_γ	> 50 MeV (for both π^0 daughters)
M_{π^0}	119 - 151 MeV
eID	> 0.001
M_D	1.68 - 2.06 GeV
ΔM	135 - 160 MeV
$P^*_{D^*}$	> 2.0 GeV

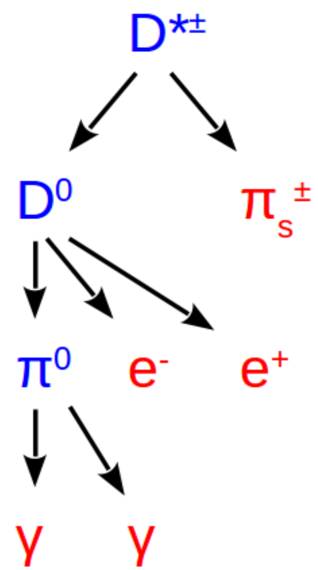

For cut optimizations, we maximize Punzi's figure of merit, using 1 stream of Y(4S) generic MC and 100,000 signal MC.

$$FOM = \frac{\varepsilon(t)}{a/2 + \sqrt{B(t)}},$$

t - cut value,
$\varepsilon(t)$ - signal efficiency for the given cut
$B(t)$ - number of background events for the given cut
a - desired confidence level in terms of standard deviations

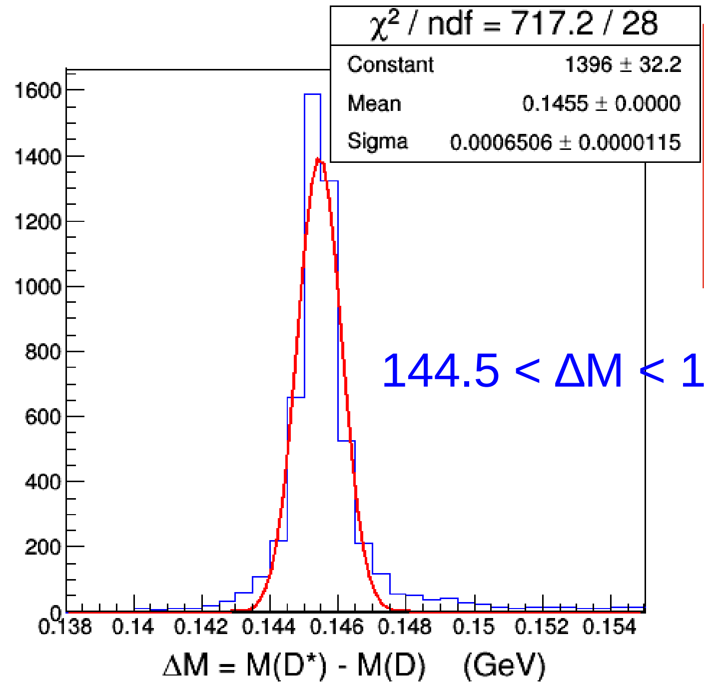

$144.5 < \Delta M < 146.5$ MeV

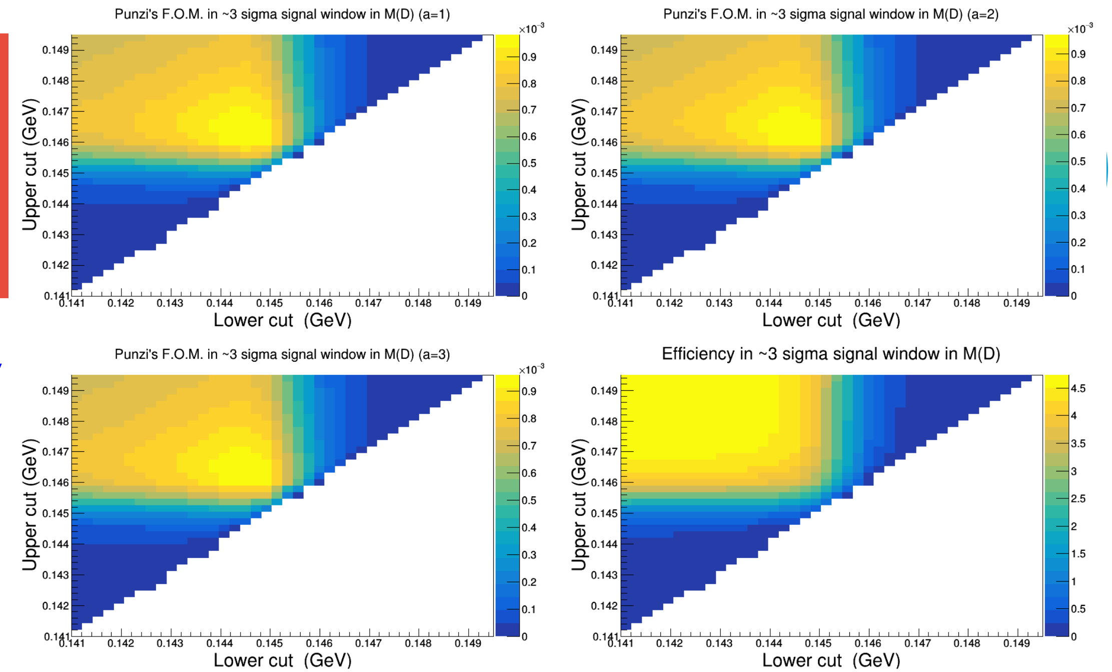

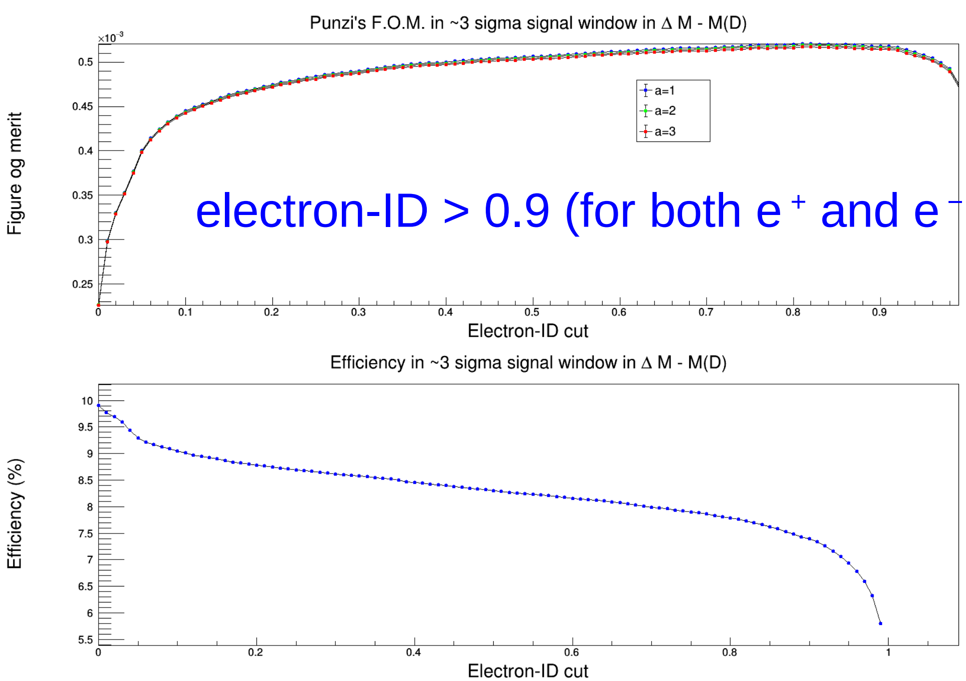

electron-ID > 0.9 (for both e^+ and e^-)

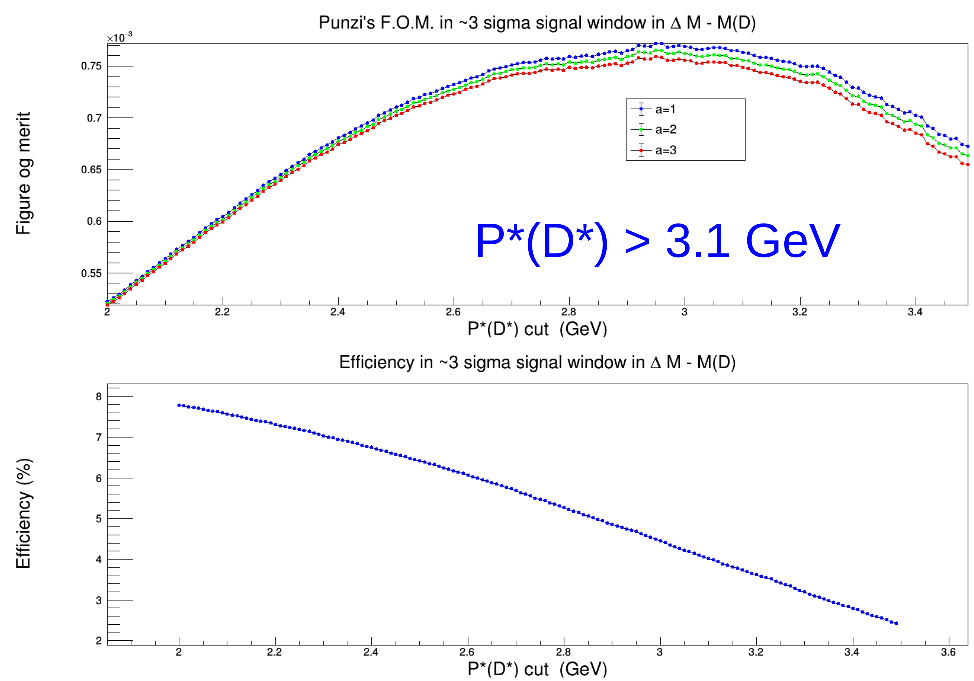

P*(D*) > 3.1 GeV

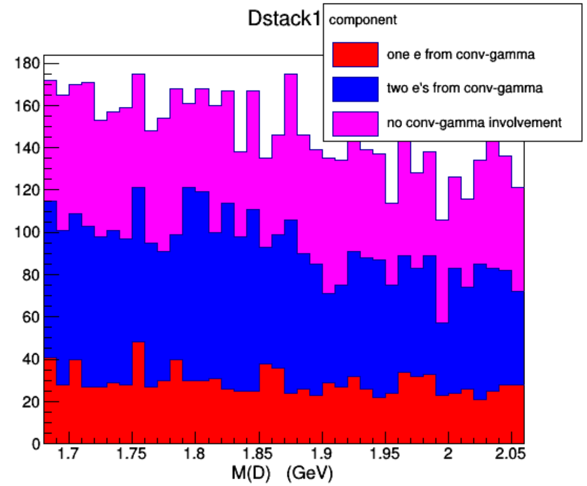

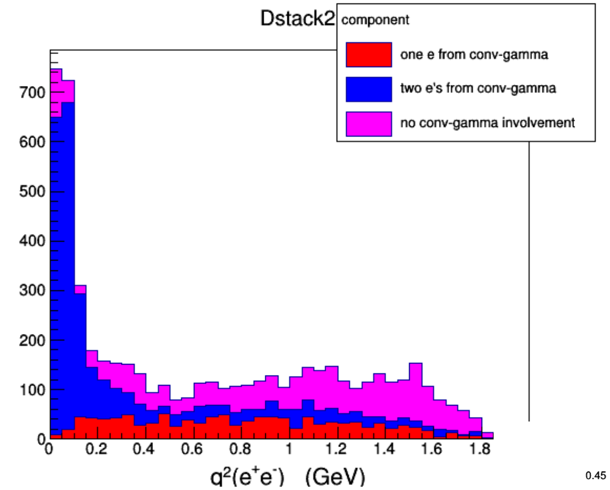

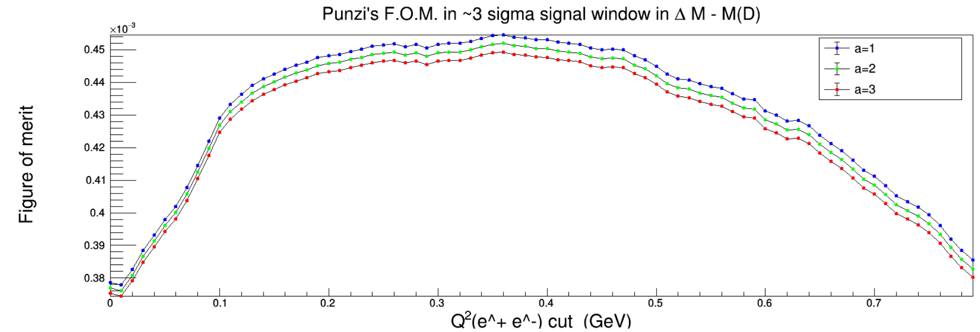

Electrons from converted photons can fake as the candidate electrons in the signal mode.

To remove this backgroung we apply

$$q^2 (e^+ e^-) > 0.35 \text{ GeV}$$

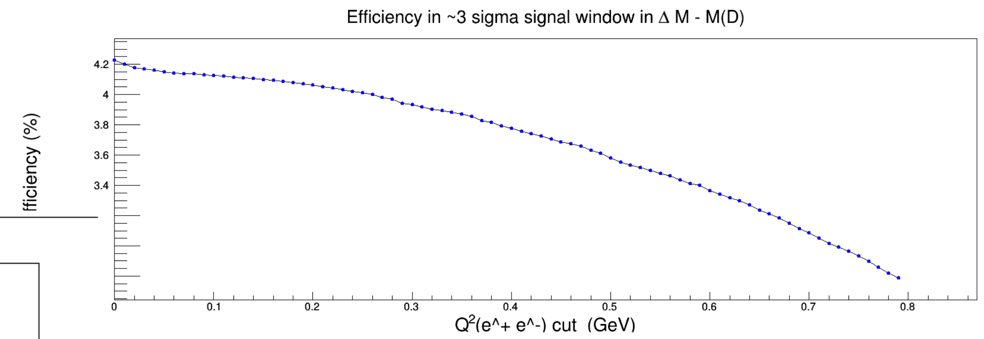

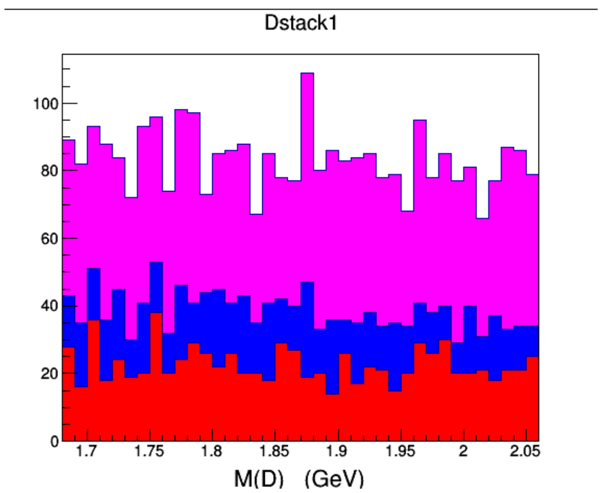

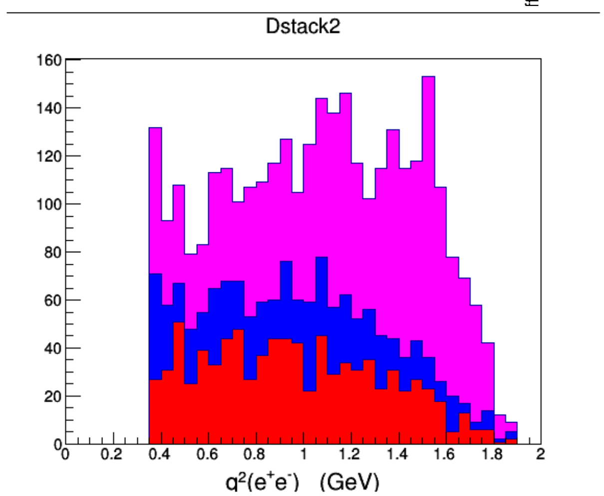

- Out of the remaining background events, a significant amount of background coming from semileptonic B − B decays.
- We train a Multi Layer Perceptron (MLP) with the first 5 Fox-Wolfram moments to dicriminate the $c - \bar{c}$ continuum from B − Bresonant backgound exploiting their different event shape topologies
- The MLP is trained and tested with B − B events from 6 streams of generic MC, and signal events from a generated sample of 100,000 MC events.

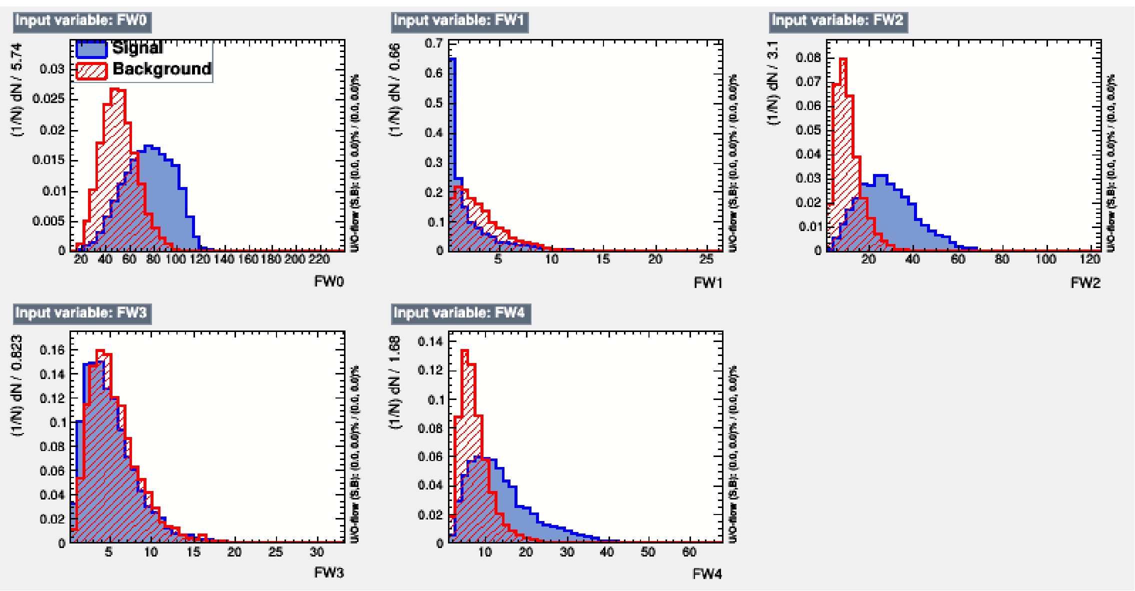

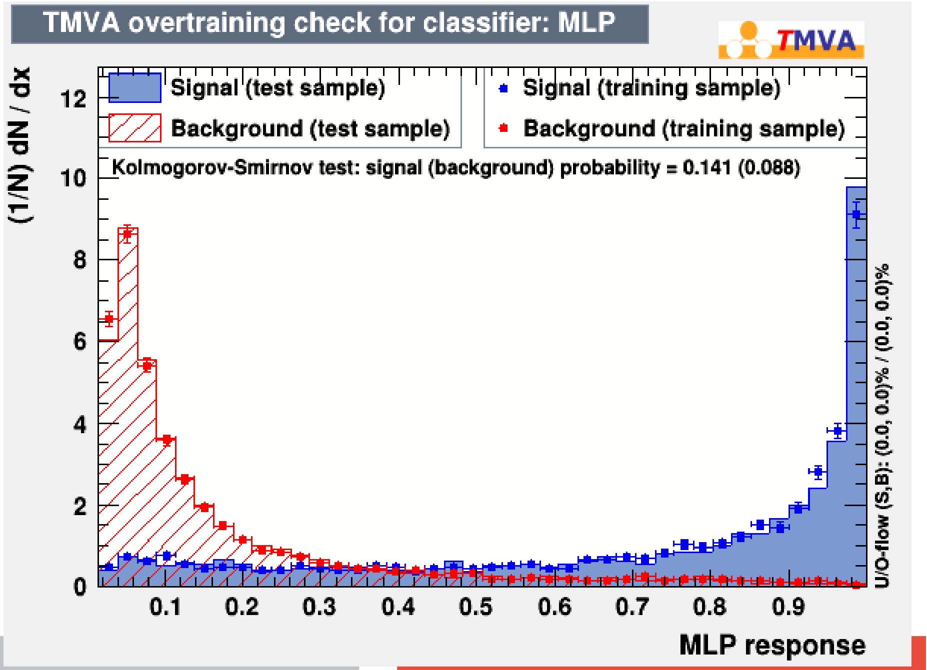

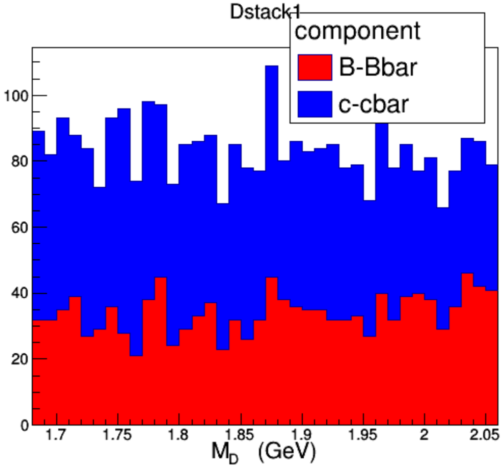

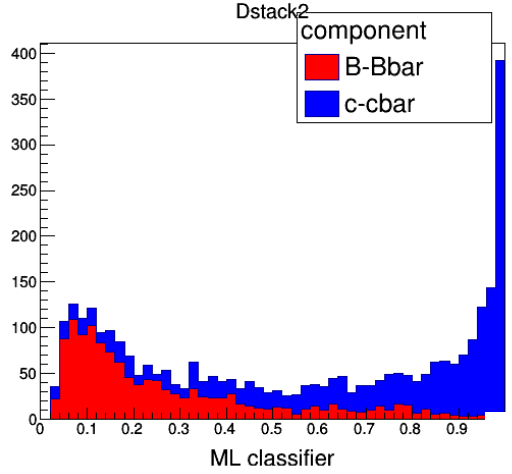

For resonance suppression,

MLP-classifier > 0.8

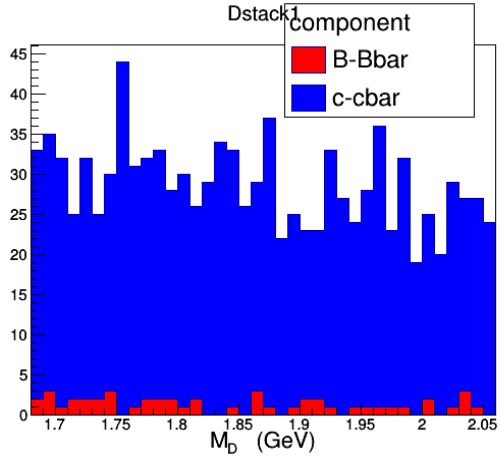

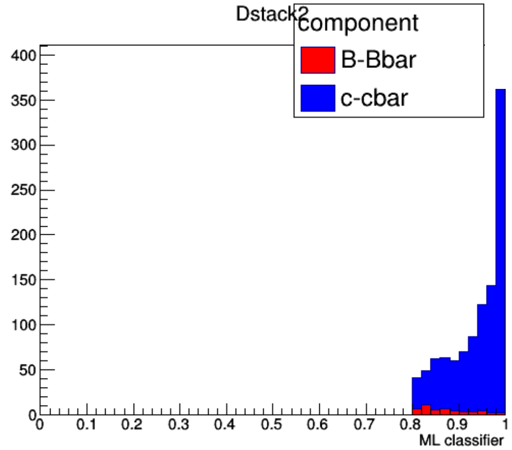

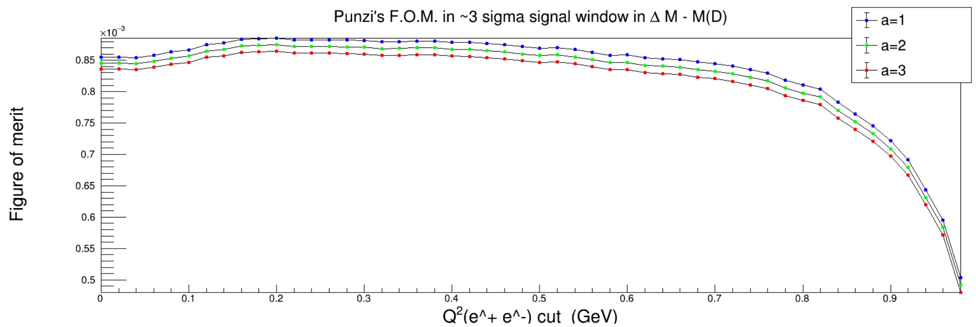

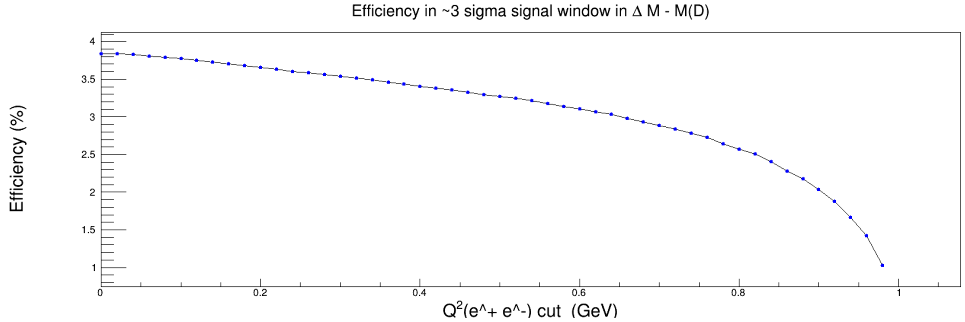

Table: Summary of cuts.

Variable	Cut
E_γ	$>$ 50 MeV (barrel ECL)
	$>$ 100 MeV (FW endcap)
	$>$ 150 MeV (BW endcap)
M_{π^0}	119 - 151 MeV
M_D	1.68 - 2.06 GeV
eID	$>$ 0.9 (optimized)
ΔM	135 - 160 MeV (optimized)
$P^*_{D^*}$	$>$ 3.1 GeV (optimized)
$q^2(e^+e^-)$	$>$ 0.35 GeV
MLP-response (Resonance suppression)	$>$ 0.8 (optimized)

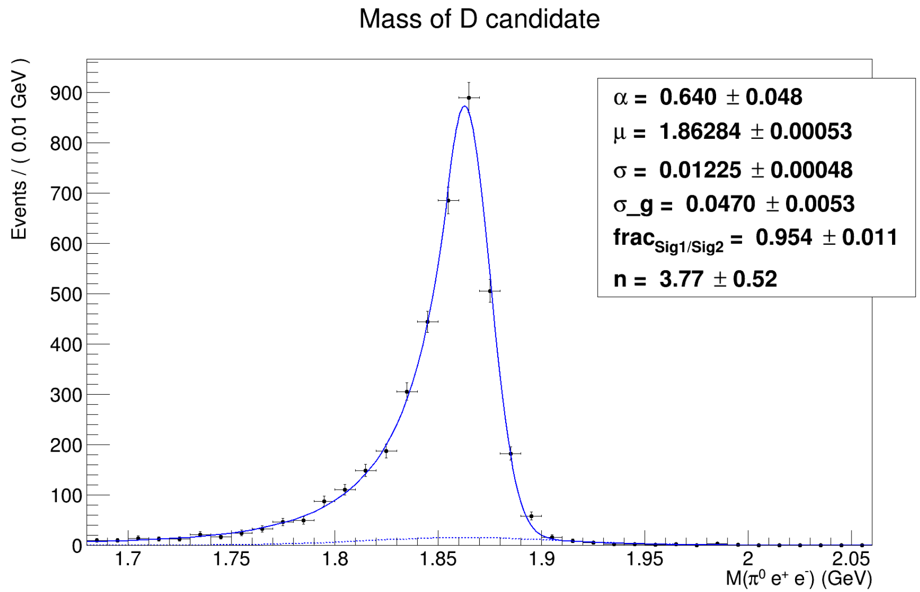

We fix the signal shape parameters (Crystal-ball function) by fitting to pure signal component from 100,000 signal MC events.

Fit to 6 streams of Y(4S) generic MC corresponding to 711 fb −1 .(contains no signal)

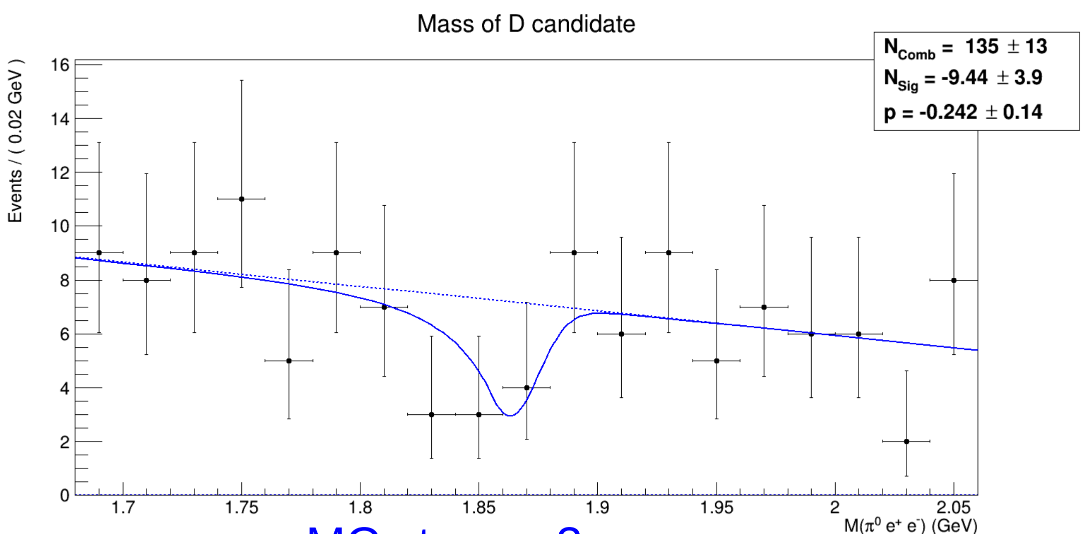

MC stream-3

Table: Fit results

MC Stream	Result
0	11 ± 17
1	-13.5 ± 17
2	20 ± 18
3	-9.4 ± 16
4	-1.3 ± 17
5	-18.3 ± 16

Sensitivity study: $D \to \pi^0 K_S^0$ as normalization mode

Table: Cuts applied.

Variable	Cut
E_γ	> 50 MeV (barrel ECL)
	> 100 MeV (FW endcap)
	> 150 MeV (BW endcap)
M_{π^0}	119 - 151 MeV
M_D	1.68 - 2.06 GeV
ΔM	135 - 160 MeV (optimized)
$P^*_{D^*}$	> 2.0 GeV (optimized)
MLP-response	> 0.8 (optimized)
(Resonance suppression)	
goodBelleKshort	= 1 (based on Belle_nisKsFinder criteria)

This mode is reconstructed with selection criteria closely matching that of the signal mode.

$D \to \pi^0 K_S^0$ yield in 1 stream of Y(4S) generic MC

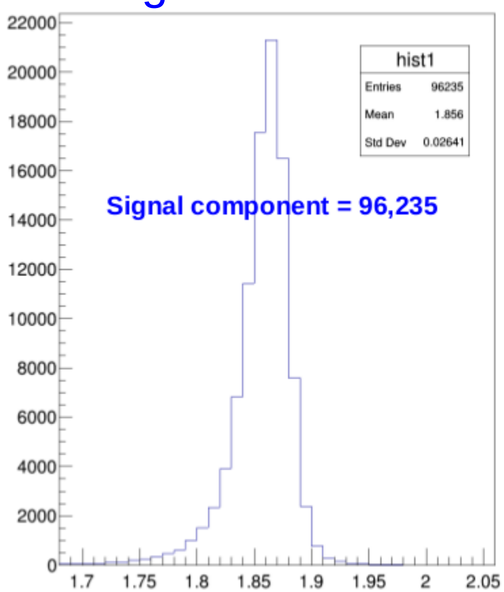

$D \to \pi^0 K_S^0$ yield in 10^6 generated signal MC events

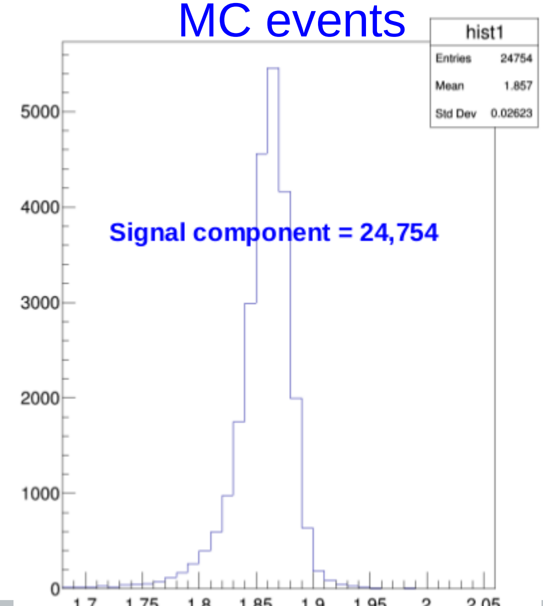

$D \to \pi^0$ e e yield in 10^6 generated signal MC events

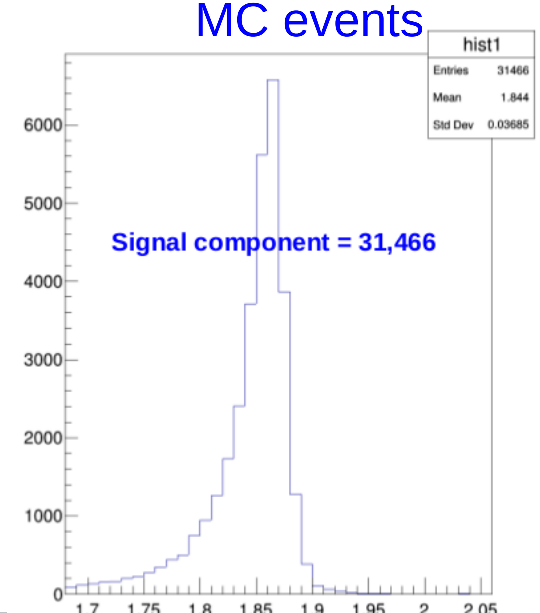

Estimating upper limit (U.L.) at 90% C.L. for Belle data

$$\frac{U.L.(\mathcal{B}_{\mathrm{D}\to\pi^0\mathrm{ee}})}{\mathcal{B}_{\mathrm{D}\to\pi^0\mathrm{K}^0_\mathrm{S}}} = \frac{U.L.(N^{GMC}_{\mathrm{D}\to\pi^0\mathrm{ee}}) \times N^{SMC}_{\mathrm{D}\to\pi^0\mathrm{K}^0_\mathrm{S}}}{N^{GMC}_{\mathrm{D}\to\pi^0\mathrm{K}^0_\mathrm{S}} \times N^{SMC}_{\mathrm{D}\to\pi^0\mathrm{ee}}}$$

$$\mathcal{B}_{\mathrm{D}\to\pi^0\mathrm{K}^0_\mathrm{S}} = 1.14 \pm 0.04$$ (PDG)

We approximate the upper limit on the D → π^0 ee yield given zero signal events as 1.6 times the uncertainty on the signal yield.

$$U.L.(N^{GMC}_{\mathrm{D}\to\pi^0\mathrm{ee}}) = \ \sim 27 \ (i.e. 1.6 \times 17)$$

Substituting numbers, the estimated U.L. for Υ(4S) Belle data (711 fb^{-1})

$$U.L.(\mathcal{B}_{\mathrm{D}\to\pi^0\mathrm{ee}}) = 2.5 \times 10^{-6} (90\% C.L.)$$

Extrapolating to full Belle data, i.e. 966 fb^{-1}

$$U.L.(\mathcal{B}_{\mathrm{D}\to\pi^0\mathrm{ee}}) = 2.5\times 10^{-6} \times \sqrt{711/966} = 2.15\times 10^{-6} \ \ (90\% C.L.)$$

Vertexing information of the e+e- tracks is expected to improve the sensitivity further.

Next steps

- **Explore sensitivity of untagged D → π^0 ee sample.**

- **Study the D → π^0 μμ mode.**
  - Significant pollution from D → π^0 π + π − expected due to pions faking as muons
  - Plan to study the fake rate using a clean control sample D → π^0 K_S^0
  - Explore possibility to improve the muon identification using via multivariate methods

Studies with displaced vertices in early Belle II data

Displaced 3-track vertices

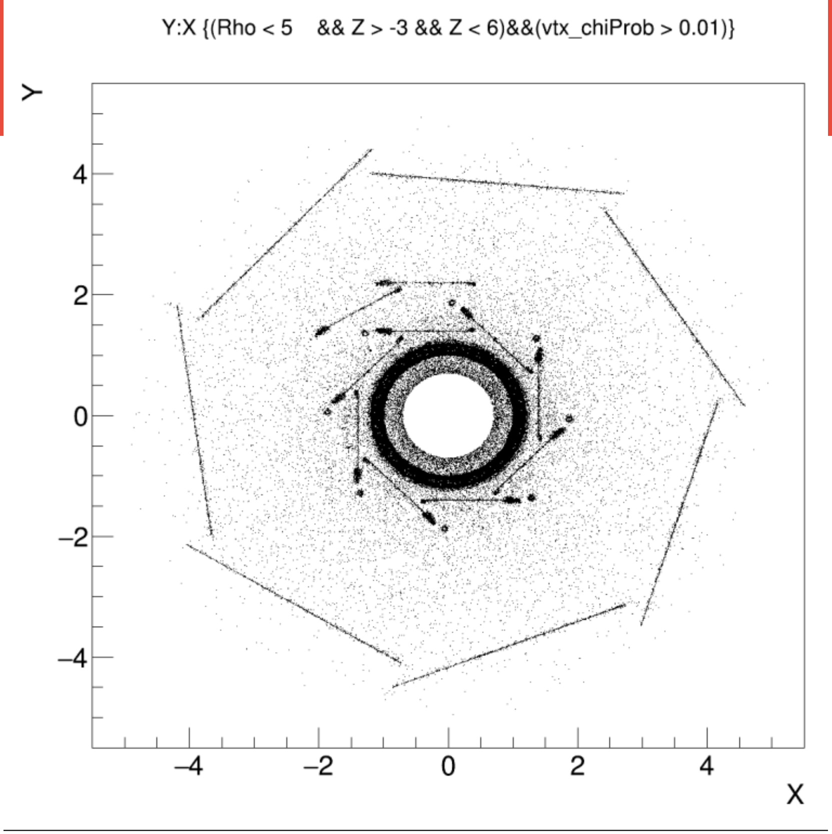

Generic MC

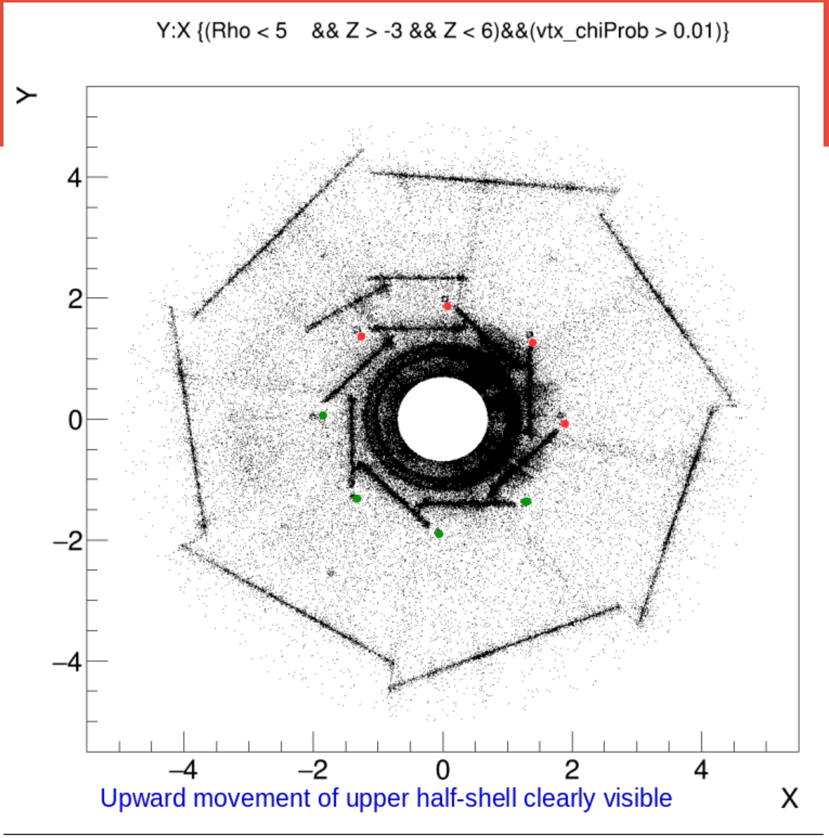

2019 Data

- Since the time when PXD was installed onto the beampipe in the KEK B4-clean room, we suspected a small misalignment in PXD half shells.
- Displaced 3-track vertices, assumed to be hadronic secondary interaction vertices, were found to provide excellent spacial resolution.
- Here, the transverse vertex density plot clearly demonstrates small misalignment in PXD half-shells

Displaced 2-track vertices

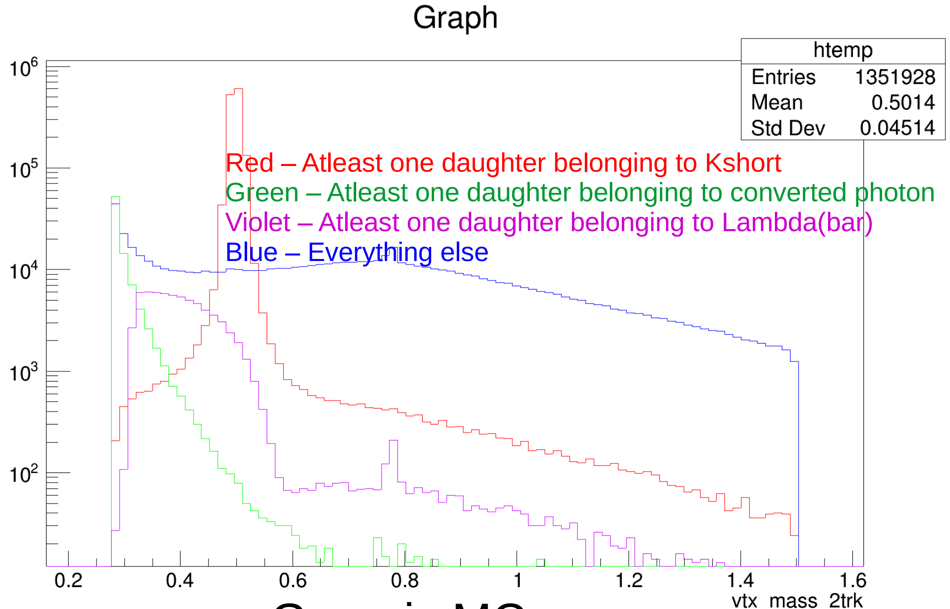

Generic MC

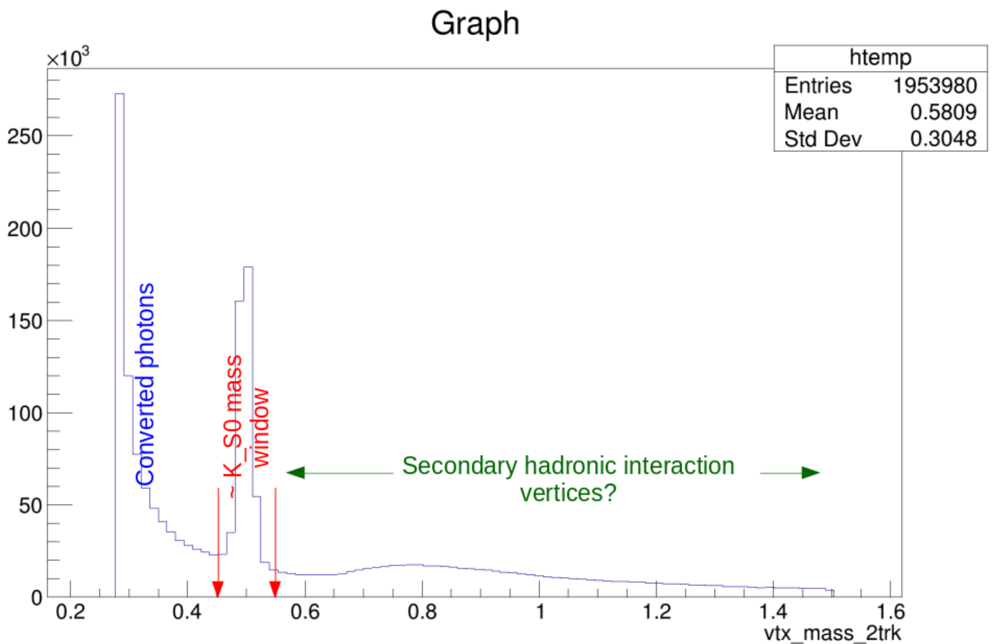

Data

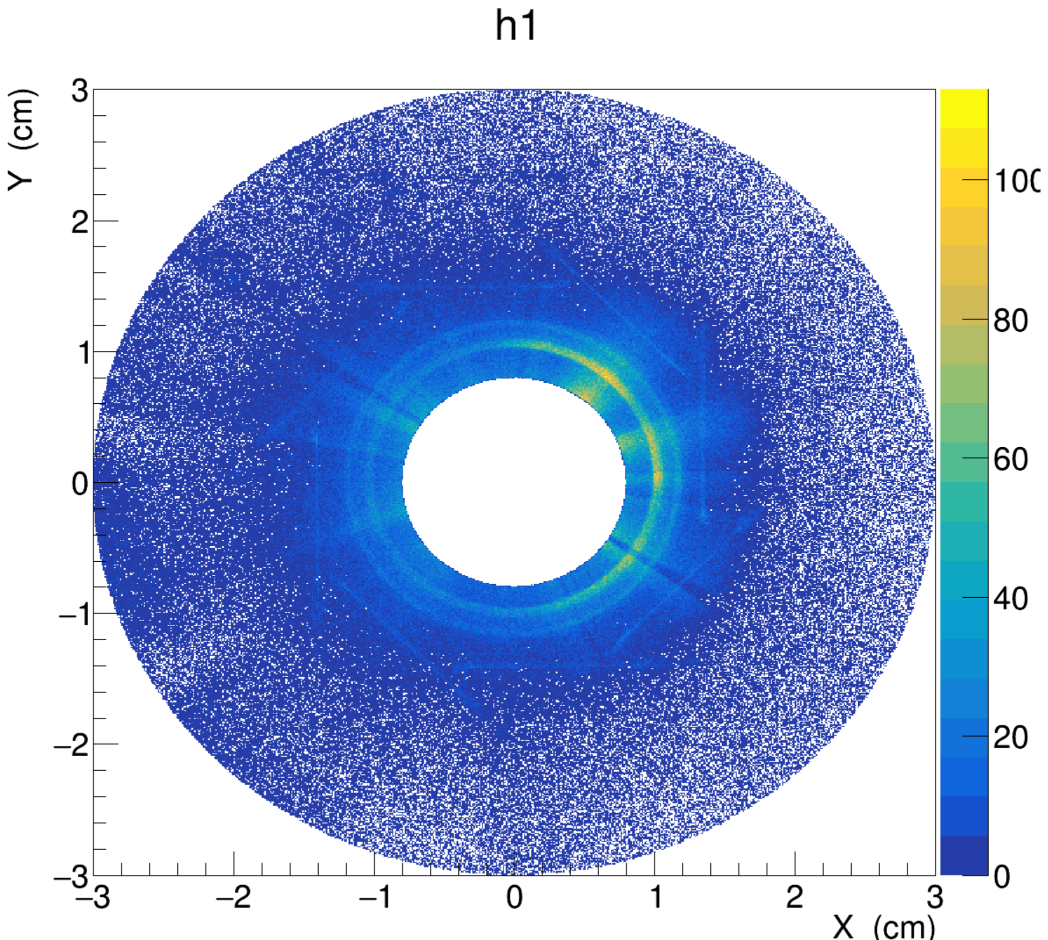

2019 Data

Apply cut : Invariant-mass > 550 MeV
Remaining displaced vertices are assumed to be mostly hadronic interaction vertices

Hotspots 2019

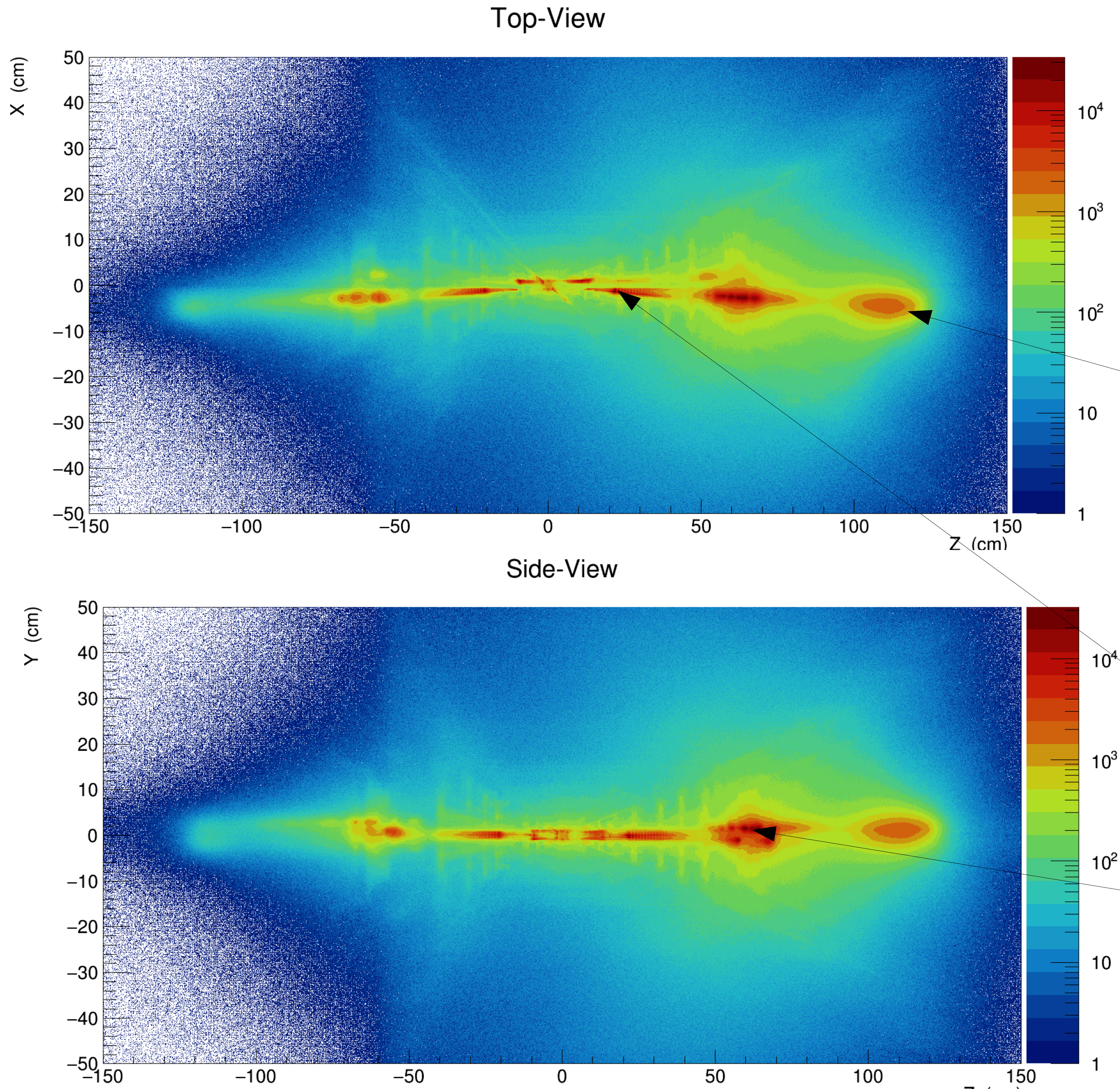

Primary showering leading to hotspots downstream?

Bellows region

LER quadrupole magnet region

Beampipe alignment

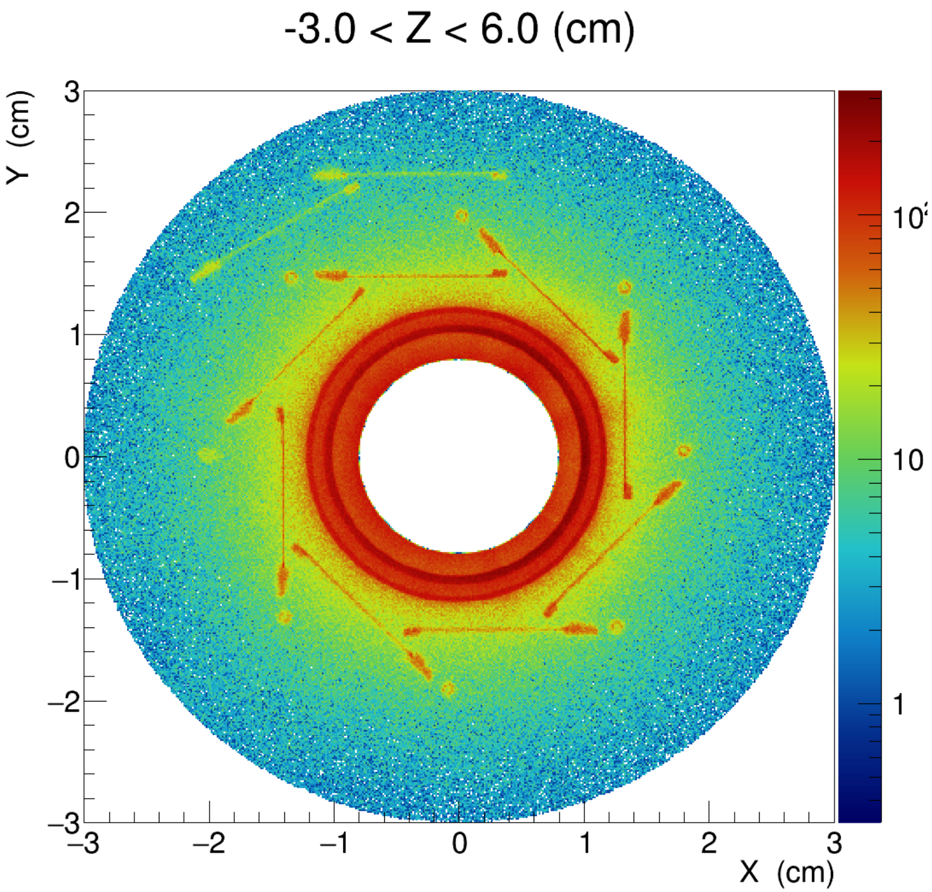

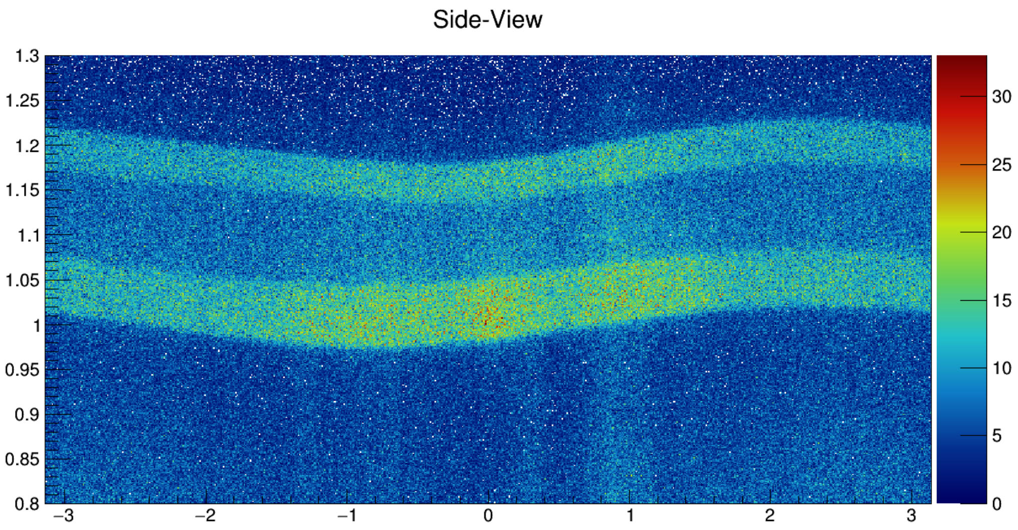

If a circle with radius R has a center displaced from the origin at (a,b) and if the displacement is small, that is
a,b >> R, then the functional dependence of the radius on the polar angle is

$$\mathbf{r(\theta) = a\cos(\theta) + b\sin(\theta) + R}$$

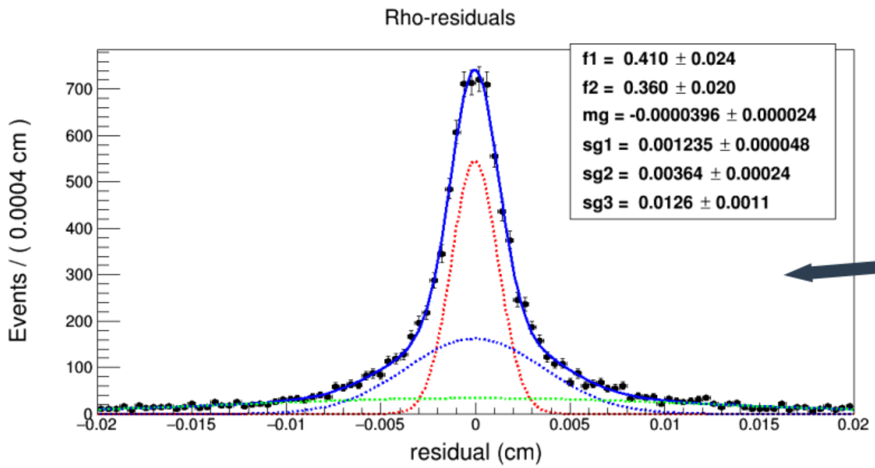

MC residuals used for convolutional fits

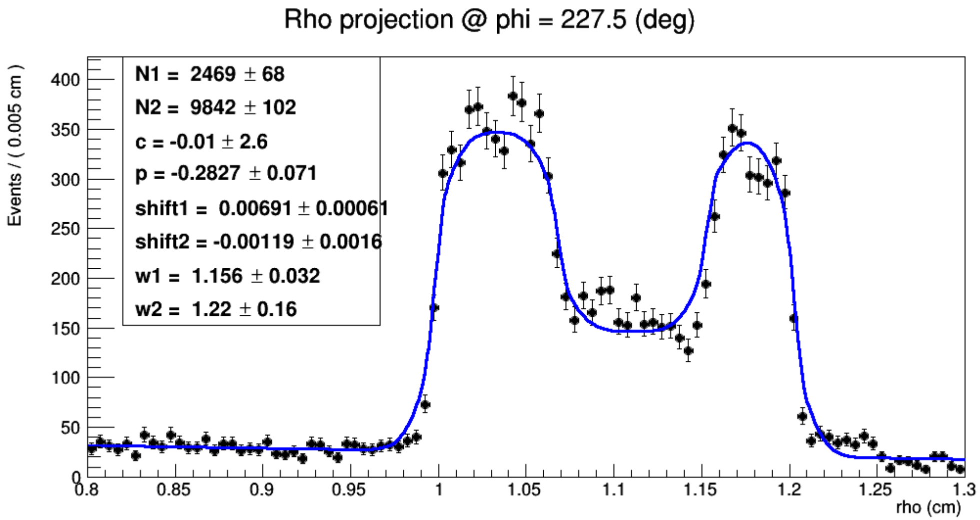

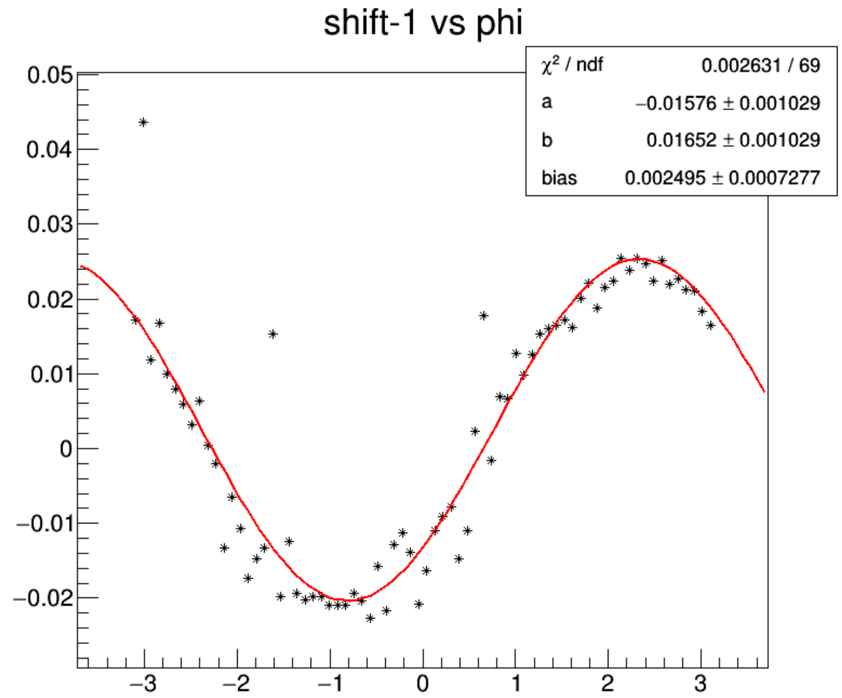

Can estimate center (a, b) by splitting the data into phi bins (5-degree bins above left), obtaining the shift from design value for each bin and then fitting the overall phi vs shifts graph (above right)

Z- dependent alignment : Divide into 20 z-bins and carry out the same exercise by simplifying fit models

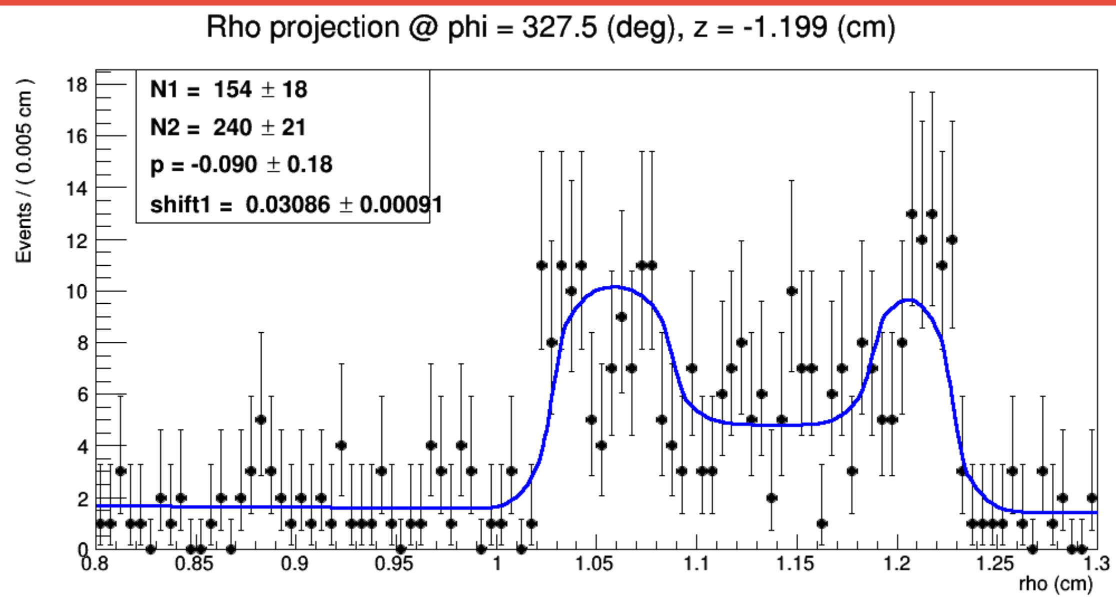

20 * 72 = 1440 raw fits such as the one on the left

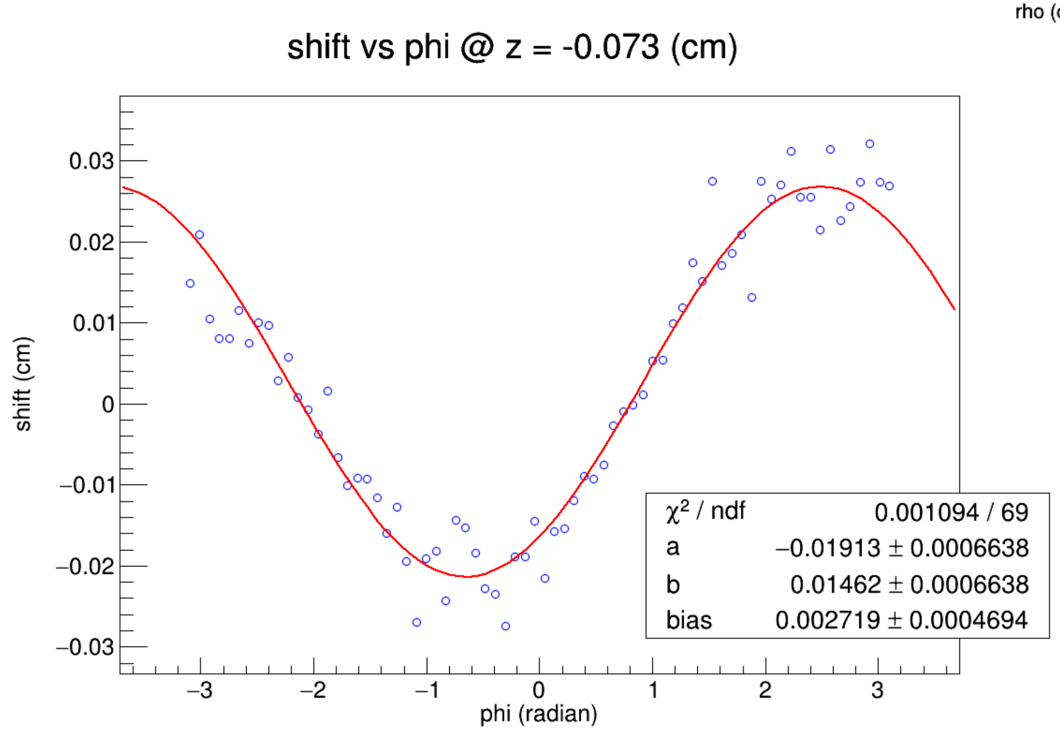

20 overall fits for each Z-bin
(e.g. left plot)

Z- dependent alignment : Divide into 20 z-bins and carry out the same exercise by simplifying fit models

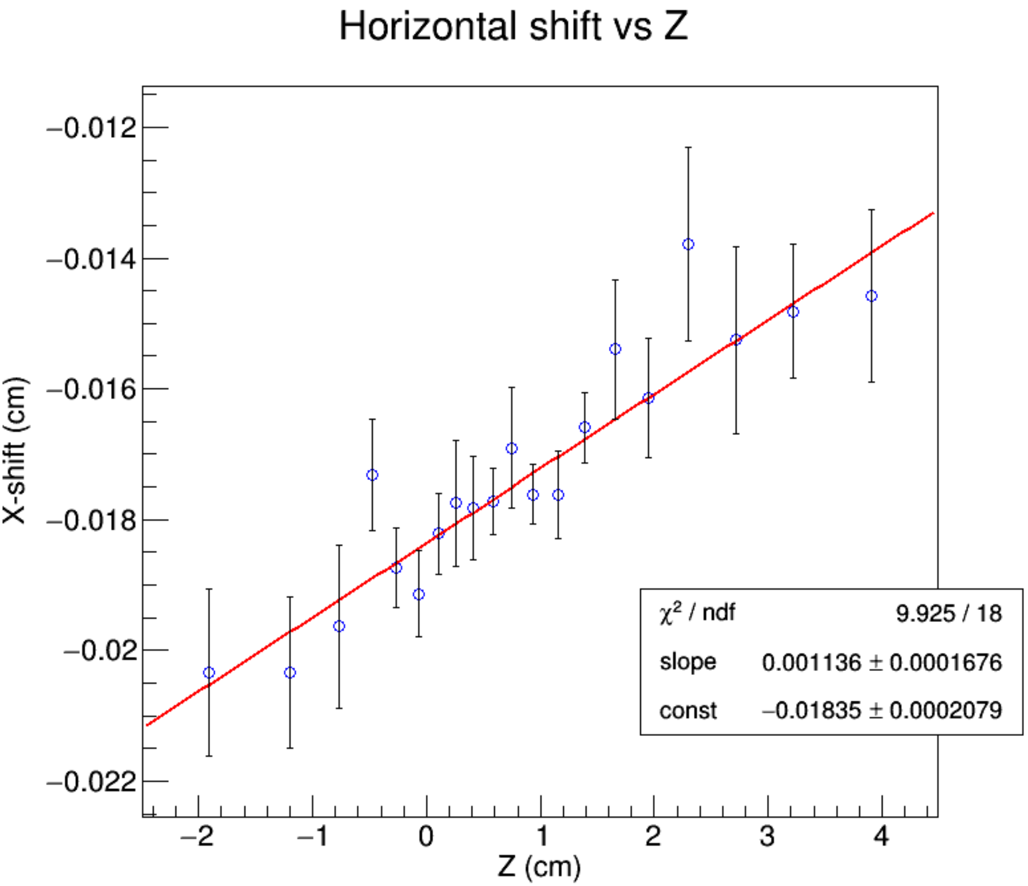

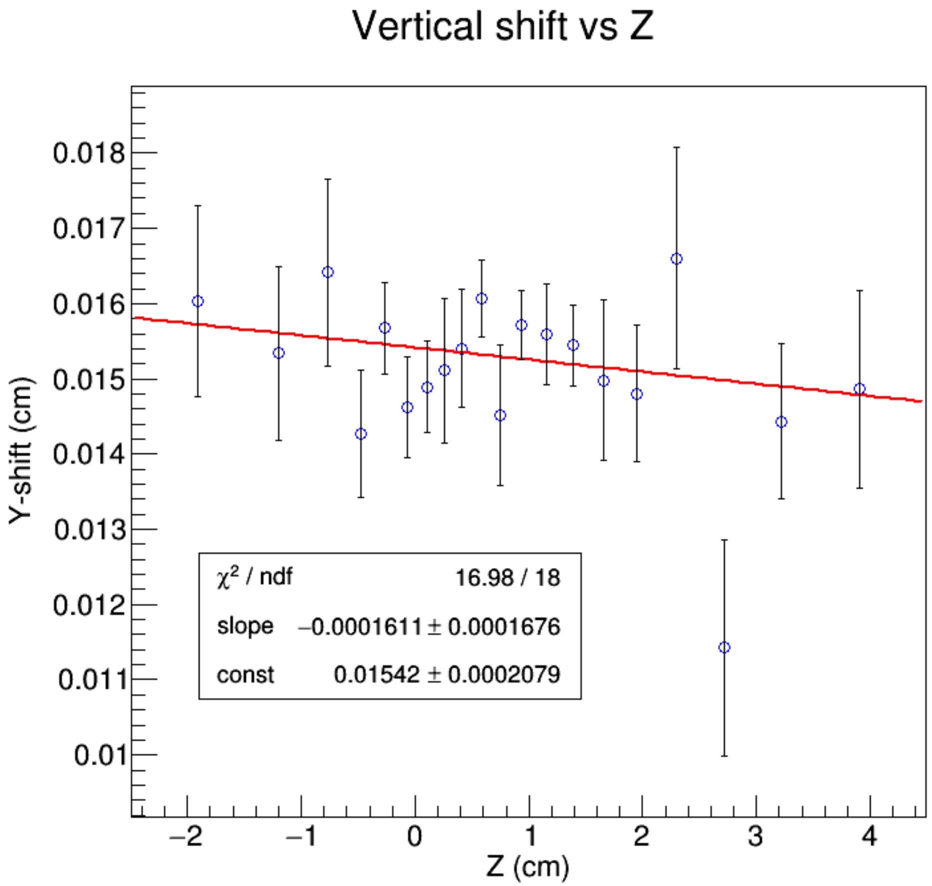

Vertical tilt : -0.0092 ± 0.0096 degrees (consistent with zero)

Horizontal tilt : 0.0650 ± 0.0096 degrees

Converted photon vertexing (presentation)

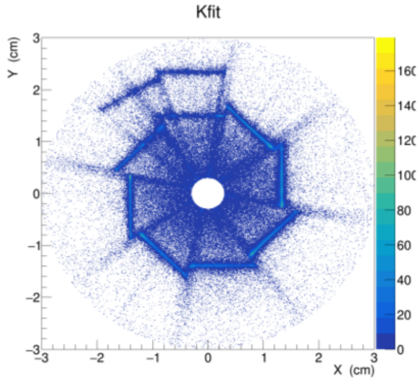

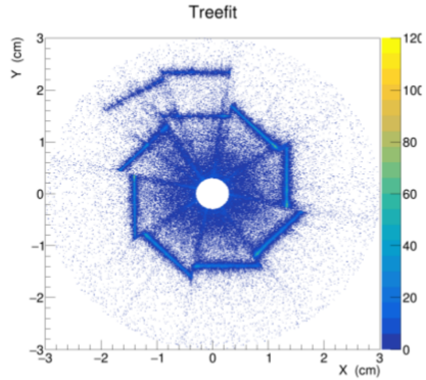

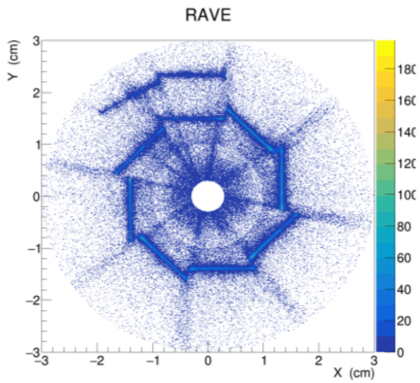

On causal inspection, RAVE seems to produce a 'cleaner' looking plot of vertex density distribution than TreeFit and KFit

chiProb > 0.2

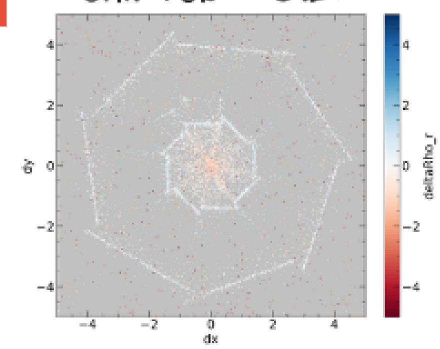

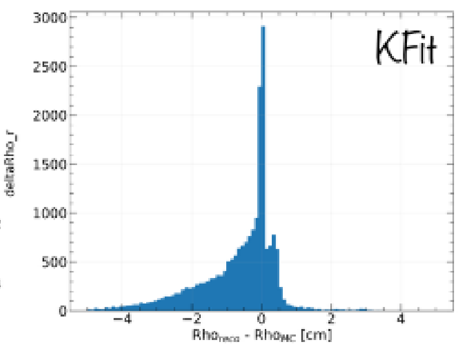

chiProb > 0.4

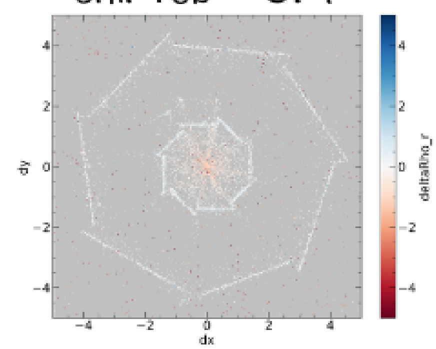

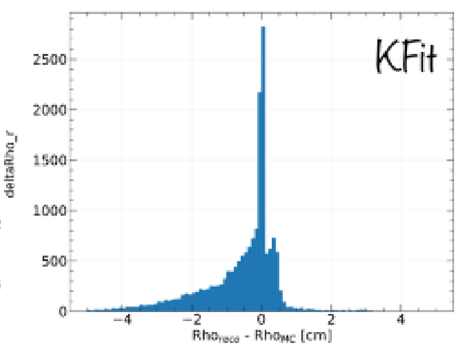

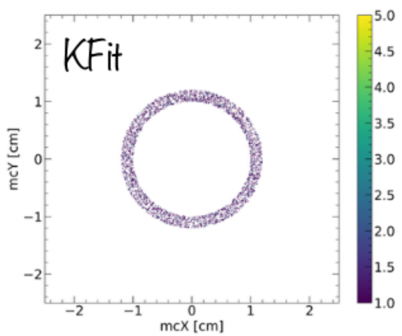

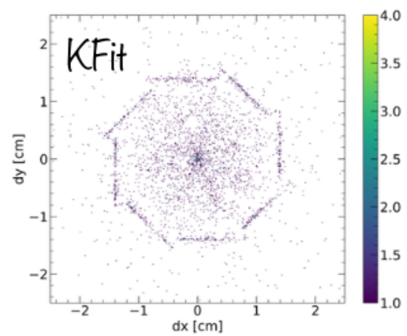

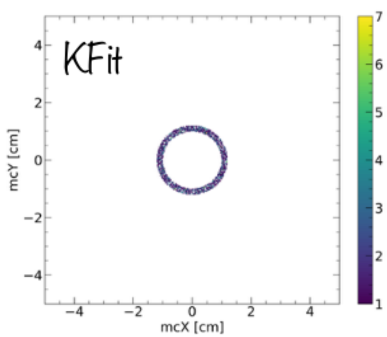

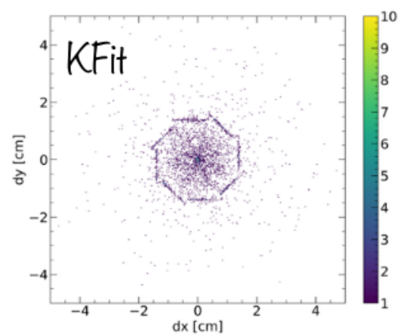

- Asymmetric ρ-residuals.
- Vertices chosen from the beampipe, when reconstructed, end up making an image of the PXD layer-1.
- Clearly demonstrates bias towards active detector material

Geometric vertex criteria

Zero opening angle

Photon conversions have the property that the momentum directions of the daughter particles are nearly parallel at the vertex.

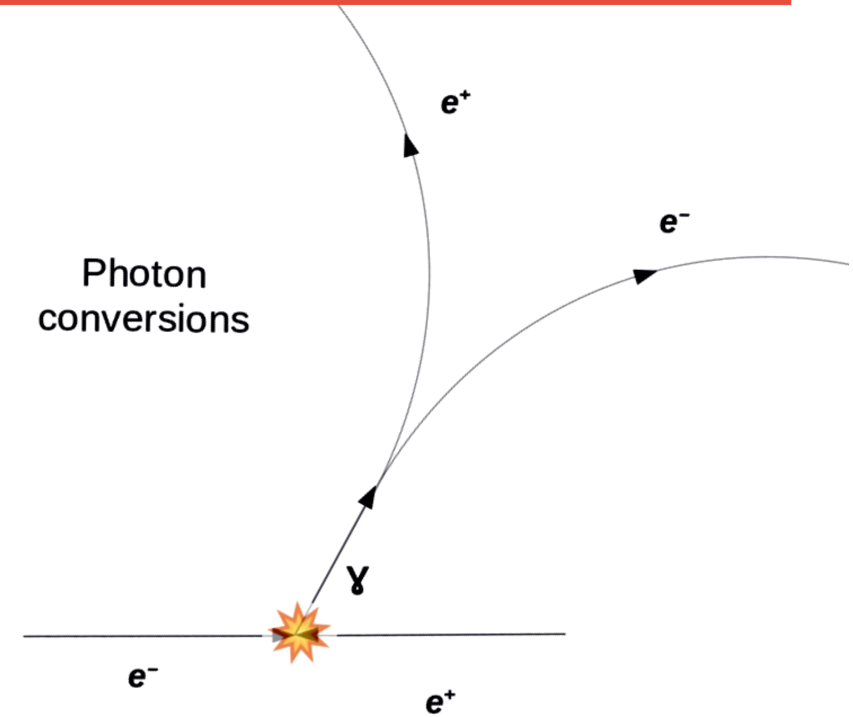

1) The zero opening angle criterion in the transverse plane implies two circles that just touch each other. In other words, the distance between the centers of the circles is nearly the sum of their radii.

$$\Delta R = |r_1| + |r_2| - |\overline{C_1} - \overline{C_2}|$$

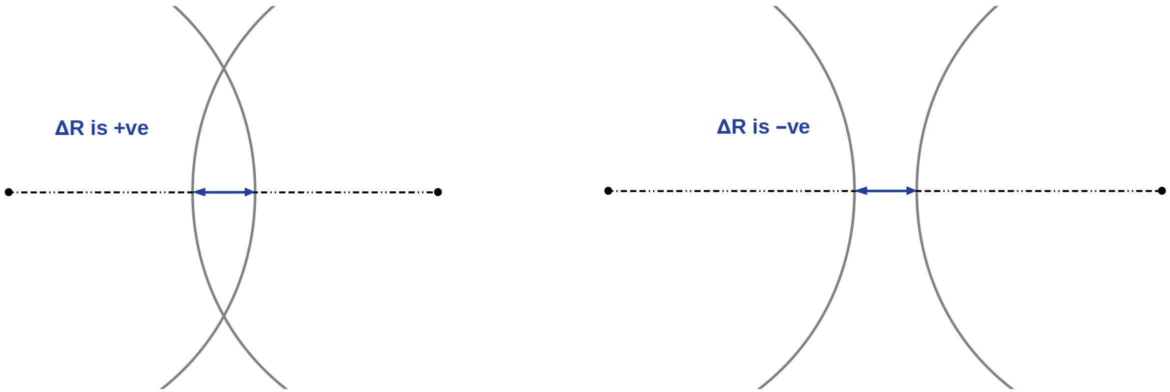

2) The next criterion is that the z-coordinates of the two tracks evaluated at their respective φ-values corresponding to the line joining their centers in the transverse plane should nearly be equal.

$$\Delta Z_{k1,k2} = z_{vtx1,k1} - z_{vtx2,k2}$$

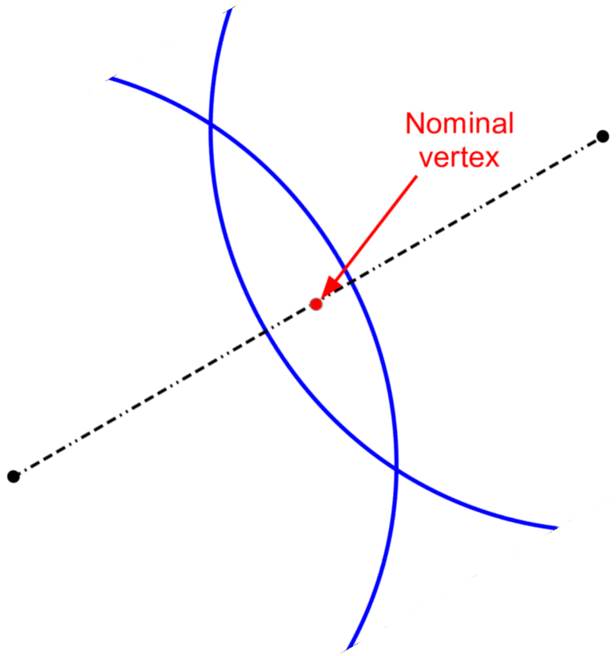

3) The tangents of the two tracks are parallel at the vertex. Matching the z-component of the unit tangents at the vertex leads to the next discriminating variable.

$$\Delta_{tan(\lambda)} = tan(\lambda_1) - tan(\lambda_2)$$

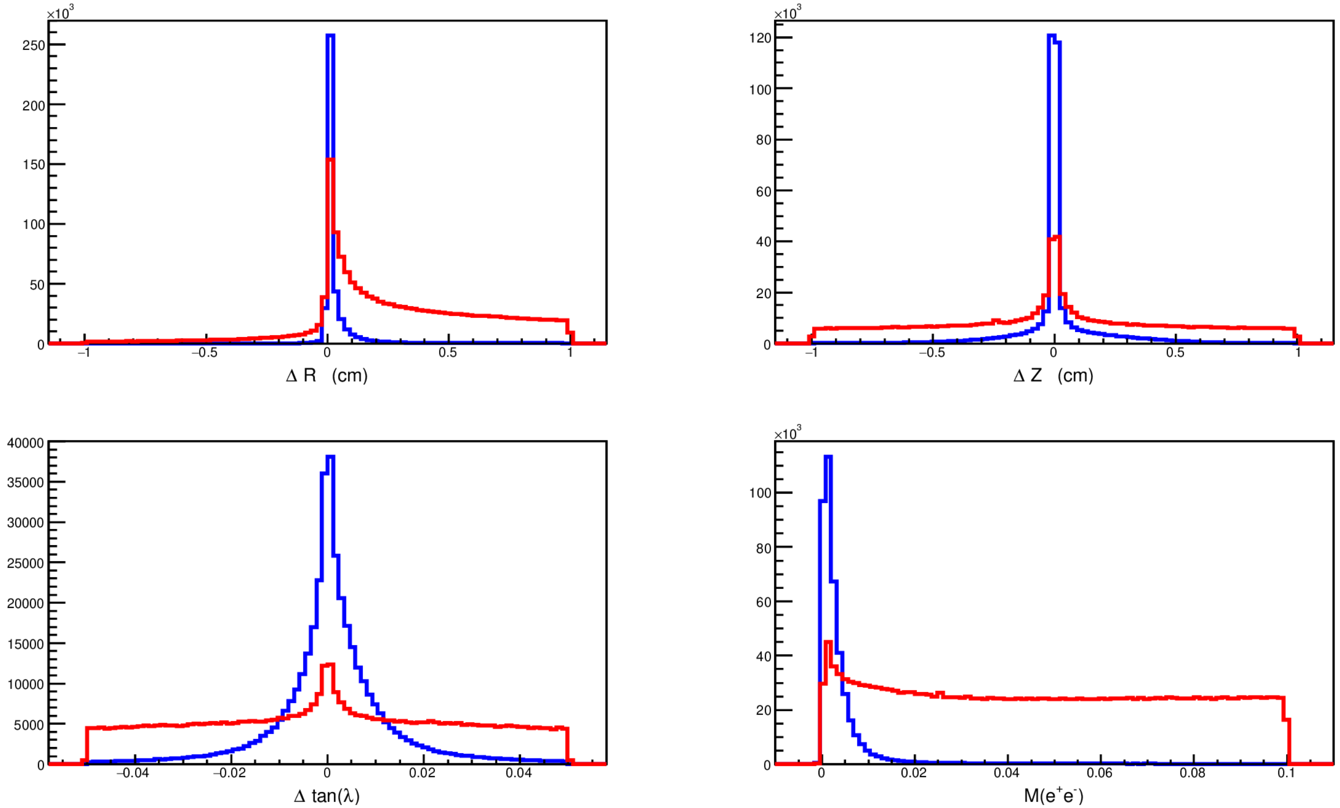

- Track objects at reconstructed mdst files can be used to construct these vertex variables.
- To test their performance against KFitt, TreeFit and RAVE, we use 10 streams of MC13b sample
- Cuts used in the reconstruction of $\gamma \rightarrow e^+e^-$ are

(i) p(e1, 2) > 0.3 GeV

(ii) χ − prob > 0.01

(iii) ρvertex > 0.8 cm

Vertex position estimation

cross section

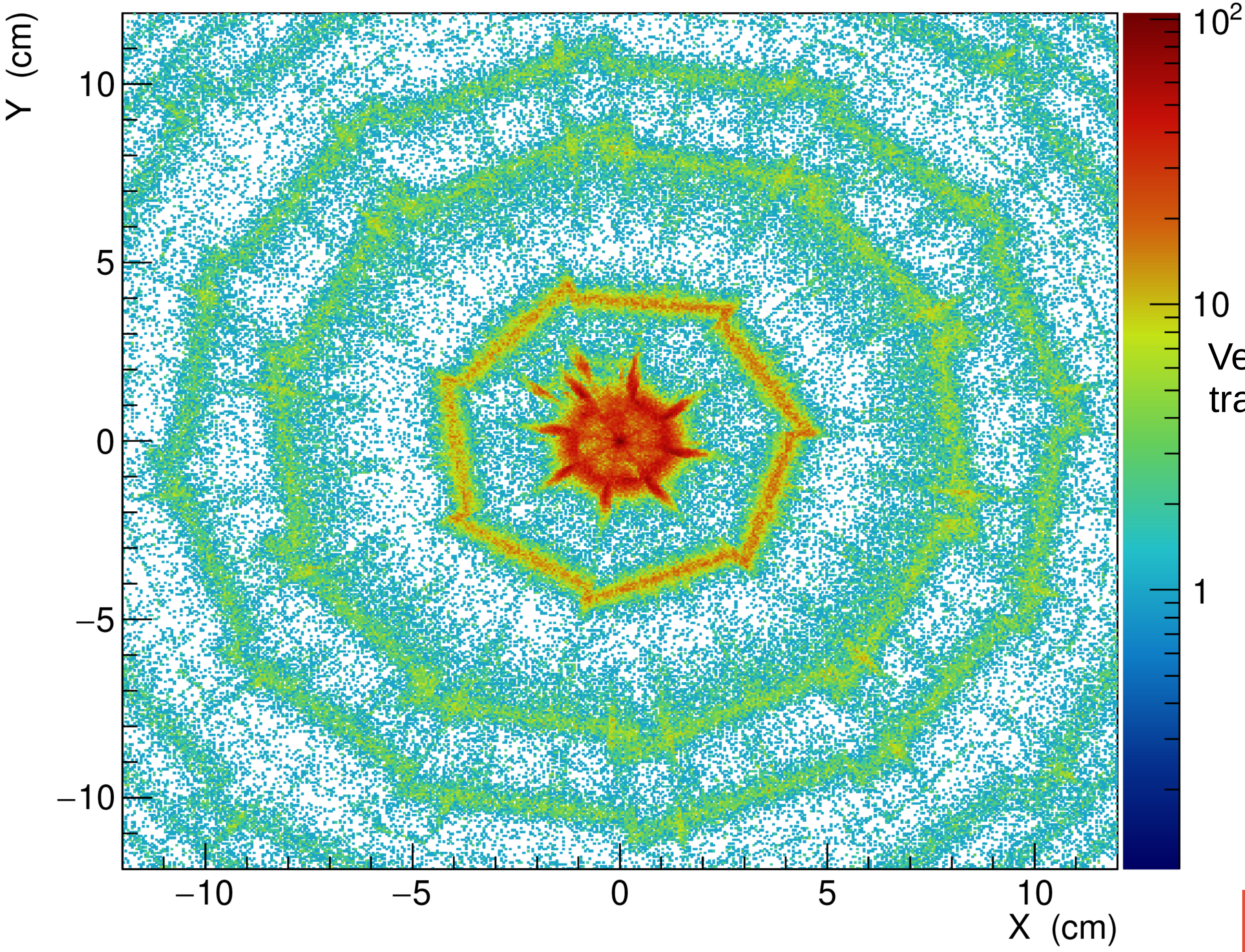

Vertex density plot in the transverse plane for truth matched signal.

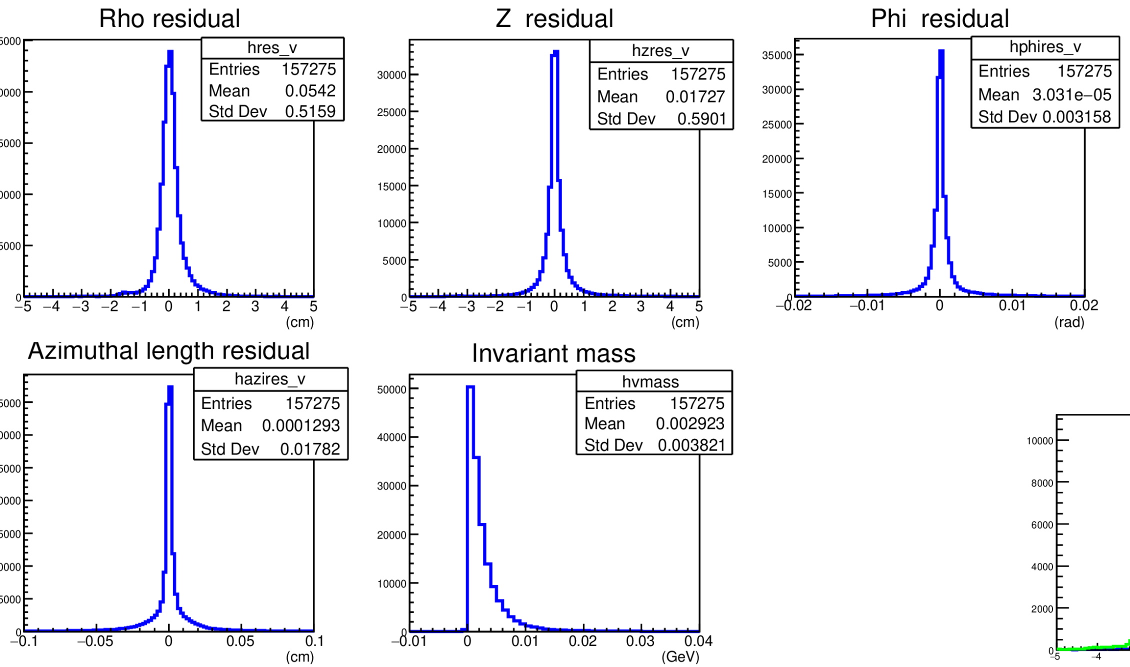

Nearly symmetric residuals

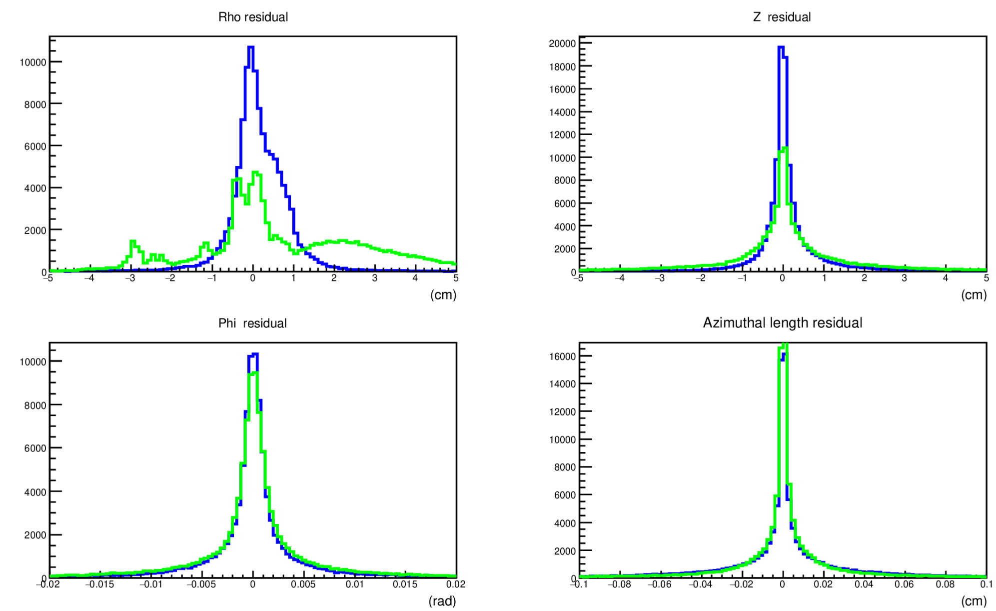

Comparison with tree-fitter residuals

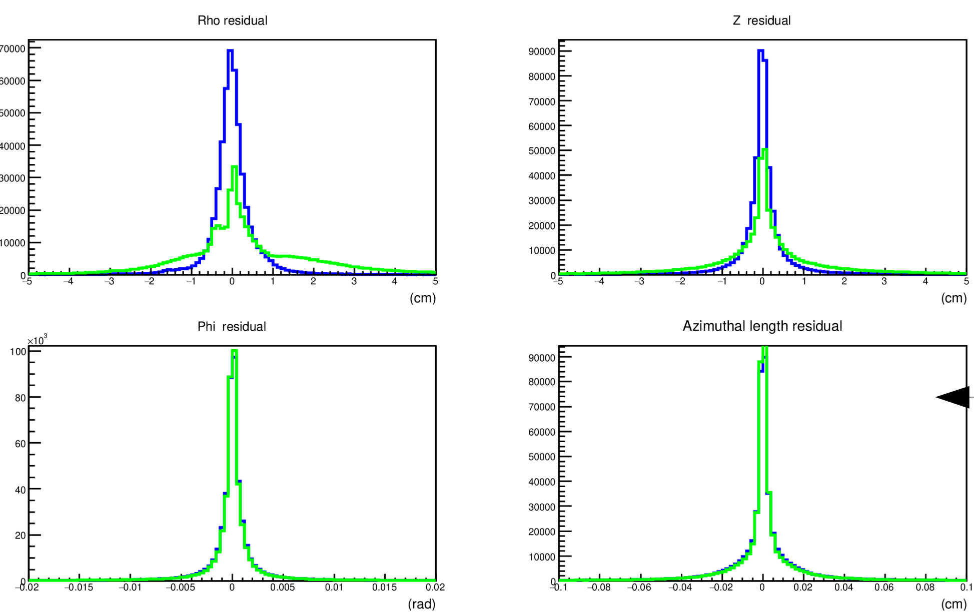

Comparison with kfitter residuals

Impact on iDM analysis signal vs. background

- iDM signal/background used to test γ-topology rejection power compared to treefit.
- To reject 50% of total remaining $e^+e^- \to \gamma\gamma(\gamma)$ background,
  - **Treefit** method requires cut of m_{V0}<0.05 GeV, corresponding **signal efficiency is 30%.**
  - γ-**topology** method requires cut of m_{V0}<0.015 GeV, corresponding **signal efficiency is 70%.**

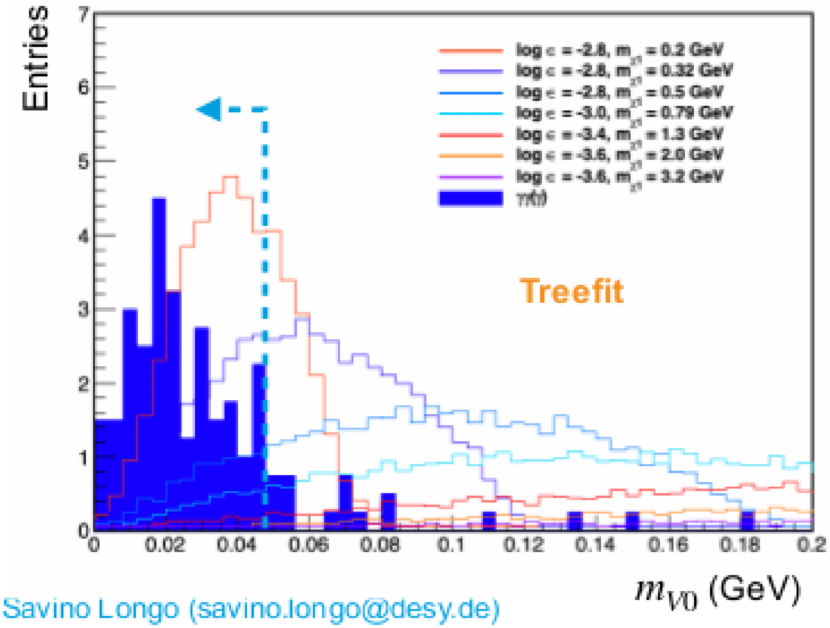

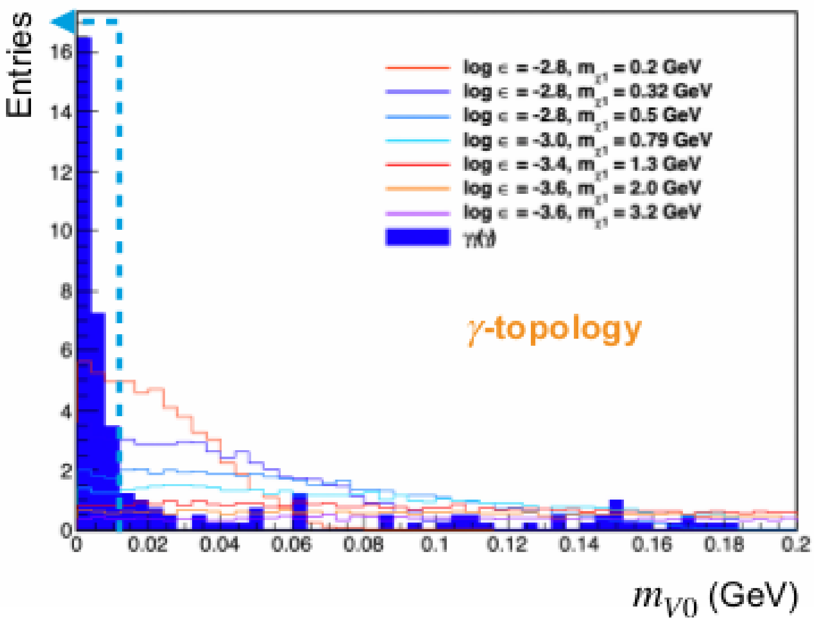

Comparing dr distribution for pointing-sample

- Significant differences in V0 dr distributions for treefit vs. γ-topology.
- γ-topology variables resolve final SVD layers and CDC wall.
- Large peak at first SVD layer with treefit is not as prominent with γ-topology variables.

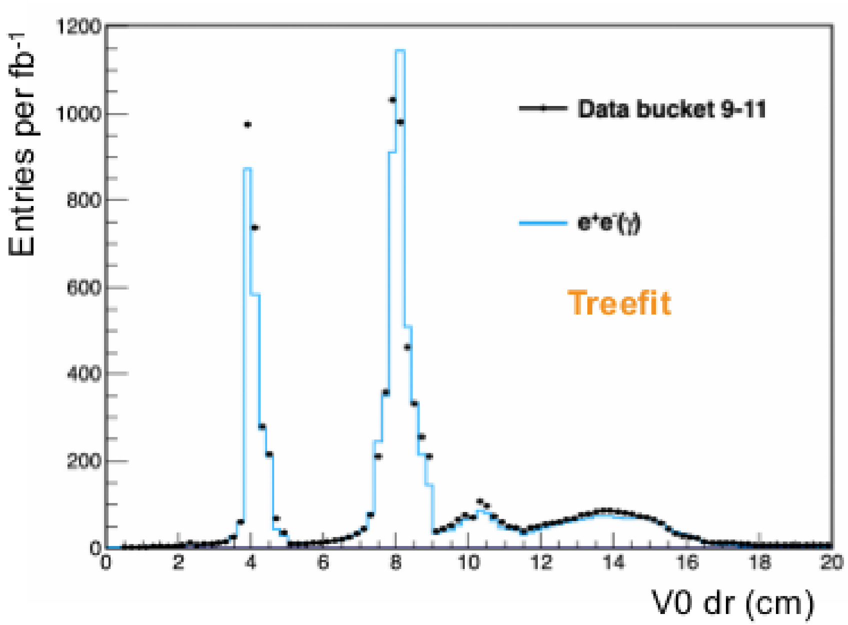

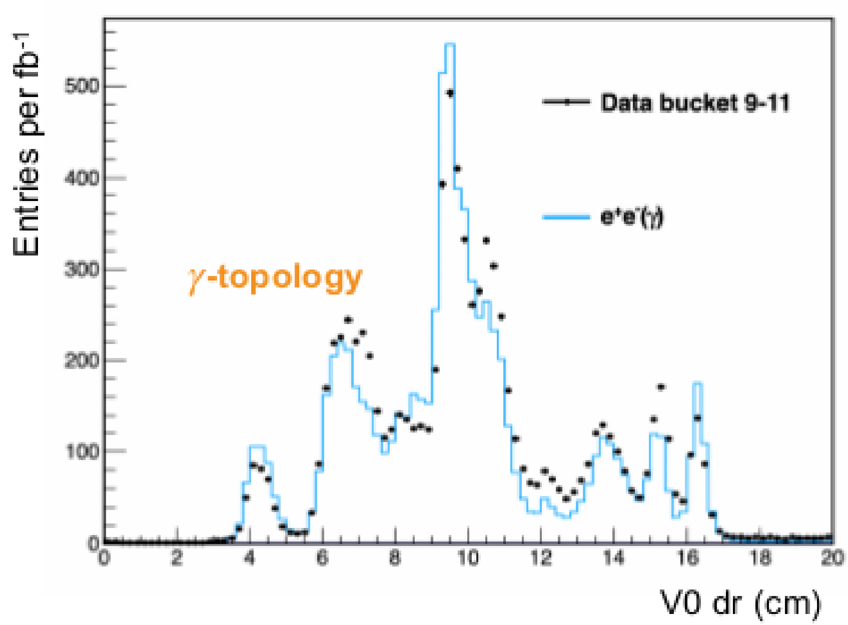

- Belle II experiment will be at the forefront of flavour physics research along with LHCb

- Collissions with $e^+ e^-$ will provide a clean environment and the large dataset that is expected in the coming years will provide a rich hunting ground for new physics

- Lot of work ahead to understand the detector and thr data it produces, on the way toward many exciting physics analyses

Thank you